International Journal of Applied Science and Engineering

Modeling the shear capacity of externally bonded fiber reinforced polymer strengthened beams by artificial neural network

Abdul Saboor Karzad[1*], Mohamed Ali Khalil[2], Abdulrahman Mostafa Mohamed[2], Samer Barakat[2]

[1] *Department of Civil Engineering, University of Ottawa, Ottawa, Canada*
[2] *Department of Civil and Environmental Engineering, University of Sharjah, Sharjah, 27272, UAE*

ABSTRACT

The current guidelines, namely ACI 440.2R and fib TG-9.3, quantify the nominal shear strength of strengthened reinforced concrete (RC) beams by simply summing up the shear strength contribution of the three components: concrete (V_c), steel stirrups (V_s), and externally bonded fiber reinforced polymer (EB-FRP) (V_f). However, as reported in the literature, this assumption is inaccurate due to an adverse interaction between EB-FRP and steel stirrups. This research study adopts a machine learning method called Artificial Neural Network (ANN) to model EB-FRP shear strength contribution. The model is built by considering the possible interaction mentioned above. Considering the collective response of these three components is crucial in accurately predicting the shear behavior because the performance potential of EB-FRP strengthening depends on the material properties of existing members. To implement the ANN modeling method, a database of 191 test specimens reported by a total of 40 individual studies is gathered. For the assessment of the proposed ANN model, a sensitivity analysis is conducted. The proposed model prediction is then compared statistically with experimental results and with the predictions of the existing guidelines such as ACI 440.2R and fib TG-9.3. The results showed that the developed ANN model could predict the EB-FRP shear strength contribution with higher accuracy than the current guidelines. Moreover, a user-modified executable program is also developed in this study to readily execute the proposed ANN model by inputting the properties of the existing beam and EB-FRP.

Keywords: Shear Strengthening, Interaction, ANN, Machine learning, Database.

Received: October 6, 2022
Revised: November 25, 2022
Accepted: December 1, 2022

Corresponding Author:
Abdul Saboor Karzad
karzad@live.com

Publisher:
Chaoyang University of Technology
ISSN: 1727-2394 (Print)
ISSN: 1727-7841 (Online)

1. INTRODUCTION

Strengthening the structures using Externally Bonded Fiber Reinforced Polymer (EB-FRP) is becoming an attractive choice for repair and/or seismic rehabilitation in the construction industry. EB-FRP strengthening technique has a wide range of applications, especially flexural and shear strengthening of beams. Since the 1990s, the EB-FRP strengthening technique has been studied and exhibited rapid growth in its application. However, among other applications, shear strengthening is a complex phenomenon and is still a matter of further research (Bousselham and Chaallal, 2006; Perera et al., 2014; Altoubat et al., 2020). When studying the shear behavior, it is widely accepted that the shear mechanism of concrete structures is a complex matter. The matter gets even more complicated by adding a new component (V_f) to the existing shear expression.

Several studies (experimental and analytical) have investigated the shear behavior of EB-FRP strengthened beams in the past two decades (Triantafillou and Costas, 2000; Chen and Teng, 2003; Ekenel and Myers, 2007; Bukhari et al., 2010; Mofidi and Chaallal, 2011; Chen et al., 2016; Karzad et al., 2017; Altoubat et al., 2018; Pujol and Marí, 2019;

Hazem et al., 2020).

Some of these studies resulted in various empirical models to predict the contribution of EB-FRP to the shear strength of the strengthened member. Some of these models are adopted by well-known organizations such as ACI and fib. The existing guidelines consider the EB-FRP contribution to the shear strength as a simple summation to their current shear expression from concrete and steel. For example, the ACI 440.2R adds V_f to their existing shear expression ($V_n = V_c + V_s$) from ACI 318 code, and fib TG 9.3 follow a similar approach by adding V_f to the current expression of shear strength from Eurocode 2 (FIB, 2001; ACI 440.2R 2017).

As widely reported in the literature, there exists an interaction between internal shear reinforcement (steel stirrups) and EB-FRP reinforcement. This indicates that the current assumption of simply adding the contribution from three components: concrete, steel, and EB-FRP to the shear strength is inaccurate. Therefore, some researchers explored this interaction and proposed new models for V_f to account for this interaction (Pellegrino and Modena, 2006; Chen et al., 2010; Mofidi and Chaallal, 2014; Ebead and Saeed, 2017; Li et al., 2018). Those prediction models are developed empirically and are based on conventional regression analysis (El-maaddawy and Chekfeh, 2012; Baggio et al., 2014; Al-Rousan and Issa, 2016; Karzad et al., 2019). As mentioned previously, shear behavior is a complex matter which may not be accurately solved using simple regression techniques. For this reason, machine learning techniques nowadays are getting more popular and can be used to tackle the modeling problem in this field.

One of the machine learning techniques called Artificial neural network (ANN) has been used in many fields and can also be used to improve the predictive capacity of the current guidelines for shear strengthening (Perera et al., 2010; Perera et al., 2014). ANNs can be implemented to solve complicated issues that conventional analytical approaches cannot handle. ANNs comprise some neurons (nodes) that interact with each other through connections with assigned weights to constitute a network. These nodes can be arranged into different layers of input, output, and hidden. Characterization of ANNs is based on an architecture and its learning mechanism (Yao, 1999). Further details about ANN are presented in section 4.1 of this paper.

The existing literature on the application of the ANNs technique in shear strength prediction of RC beams strengthened using EB-FRP (Tanarslan et al., 2012; Bashir and Ashour, 2012; Hosseini, 2017; Jumaa and Yousif, 2018) is not adequate to fully address the interaction-related concerns. The existing literature about ANN modeling of EB-FRP shear strength is focused on the beams without any shear reinforcement (which is not recommended by the current standard codes for design and construction), or they combined the two different configurations of EB-FRP strengthening (U shape and full wrapping) in the modeling process. The latter combination will not give the full picture of the matter as the full wrapping does not primarily fail due to debonding while it is the dominant and the concerning mode of failure in U shape configuration.

The objective of the current research study is to propose an ANN model for predicting the shear capacity of EB-FRP strengthened RC beams. The beams included in the study contain at least a minimum amount of conventional shear reinforcement (steel stirrups) and are strengthened either by a U-shape or side bonded EB-FRP. To that end, an experimental database consisting of 191 RC beams test results was compiled from existing literature. Using the collected database, an ANN model was built by considering the materials-related and geometry-related parameters. In developing the ANN network, a total of 16 parameters were considered as input nodes.

2. METHODOLOGY FRAMEWORK

The methodology framework consists of four stages (see Fig. 1). At stage one, the data about tested beams, including their characteristics and performance, was collected from literature to use in the ANN modeling process. More than 40 articles were reviewed, and the data was retrieved and stored. The criteria for retrieving the data included RC beams with EB-FRP, the existence of the shear reinforcement, and the load configuration (i.e., simply supported three or four points loading). In stage two, the model development and testing were executed. Given the widespread use of the ANN technique and its proven performance over many other methods, it was adopted for modeling purposes. Several ANN model architectures were attempted to best fine-tune the model to favor our prediction purposes.

Furthermore, the best ANN model was compared with other conventional models for predicting V_f, including ACI 440.2R and fib TG9.3. At stage three, a sensitivity analysis was conducted using the ANN model to reveal the interrelation between the dependent variable (the V_f) and the other independent variable. This stage was essential to give the reader further in-depth dimension about the relationship between the variables in real life. Finally, a standalone application was developed to integrate the best ANN model to ease the process of V_f prediction to other interested researchers and practitioners.

3. DATABASE COLLECTION

A literature review was conducted extensively to collect enough data points. Also, previously published databases have been reviewed (Sas, 2011; Barakat et al., 2019), and as a result, a database of 191 strengthened RC beams test results was retrieved from the literature (see the appendix for details). The database contains RC beams with internal steel stirrups strengthened in shear with EB-FRP. Since the beams without steel stirrups are not recommended by the standard codes in practice (e.g., ACI 318), only beams with conventional shear reinforcement (steel stirrups) are considered in the current database. The collected data were about simply supported conventionally reinforced beams tested under three points loading or four points loading. The samples collected present a high diversity containing slender beams, short or deep beams, T beams, Rectangular beams, and beams with different concrete compressive strength but higher than 20 MPa. Based on the codes and the literature, concrete compressive strength lower than 20 MPa is not advised as structural concrete.

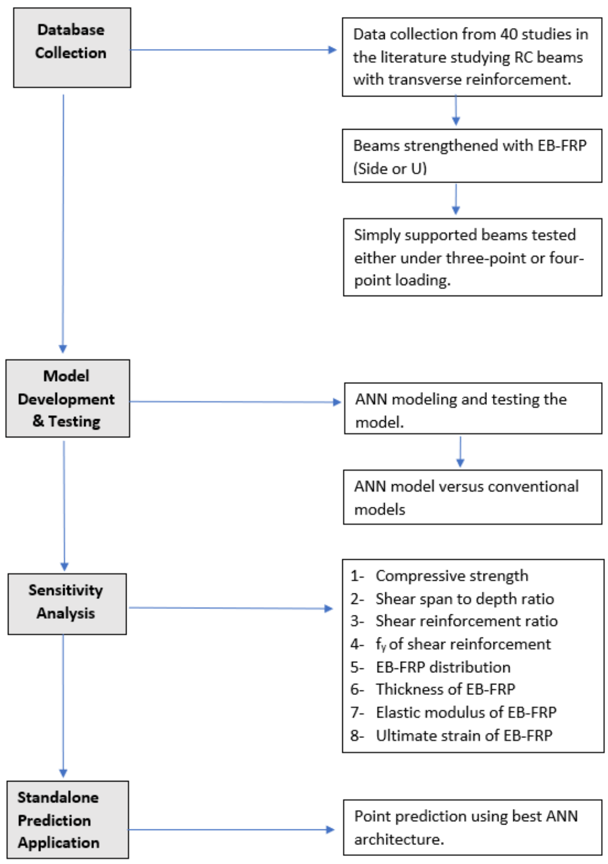

Fig. 1. Methodology framework

All the samples collected in the database are strengthened either with carbon fiber reinforced polymer (CFRP) or glass fiber reinforced polymer (GFRP) sheets. Only two types of EB-FRP strengthening configuration are included in this research: side bonding and U jacketing (with and without anchorage). Because side bonding and U jacketing strengthened beams exhibit similar failure modes where debonding is the dominant failure mode. The collected database reports all the properties, including the geometry of the beams, materials properties, reinforcement details, and test results of the samples. The variables gathered in the database are the compressive strength of concrete, cross-sectional properties of the beams, shear span-to-depth ratio, mechanical and geometric properties of EB-FRP materials, longitudinal and transverse reinforcement properties, and finally, the contribution of EB-FRP to the shear strength (V_f).

The reported specimens in the database were made of concrete with a compressive strength of 20 to 60 MPa. 33% of the beams have 20 MPa < f_c' < 25 MPa, 57% of beams have 25 MPa < f_c' < 45 MPa and 10% of beams have 45 MPa <f_c' < 60 MPa. This wide range of concrete strength covers the old concrete f_c' < 25 MPa, which is the case in rehabilitation application, conventionally used concrete 25 MPa < f_c' < 45 MPa and relatively high strength concrete f_c' >45 MPa, which can be the case for strengthening application. 40% of the beams have a T-section, and the remaining 60% have a rectangular cross-section. Both slender and short beams are included in the database, with 23% of short beams and 77% of slender beams.

The beam specimens included in the database are strengthened with either CFRP (C) sheets or GFRP (G) sheets. Only 8% of the beams are strengthened with GFRP sheets, and the rest are strengthened with CFRP sheets. The continuous (Ct) and discrete (Dt) distributions of EB-FRP strengthening reported in the database comprise 43% and 57%, respectively. The majority of the specimens included in the database are strengthened with a vertical inclination (90°), and 4% of reported specimens have an inclined configuration strengthening application. The debonding failure mode (DB) was prevalent among the specimens reported in the database. The beams that exhibited rupture failure (RT) of the EB-FRP sheets are 18% of the total specimens. One-fourth of the samples with EB-FRP showed a strength increase of around 50%.

It was evident from the literature that conducted experimental studies followed procedures more representing strengthening with very few studies on the repair. Almost all the studies did not involve sustained loading or pre-loading condition to cause noticeable damage that results in loss of original capacity. While in reality, the member in need of repair or strengthening will be subjected to some extent of sustained loading and the presence of some level of damage which can be a highlight for further investigations.

Fig. 2 presents a visualization of the data distribution in the collected database. The distribution histograms plotted in the Figure are only for the parameters used as input variables for ANN modeling. However, the number of variables reported in the database is 31 consisting of all the geometric and mechanical properties of the components of the beams (concrete, steel, and EB-FRP). The histograms illustrate the number of papers in the database that reported the same value of a specific parameter. For instance, there are 50 papers (Frequency 50) in the database that reported beams with f’c of 25 MPa as shown in the first histogram of Fig. 2.

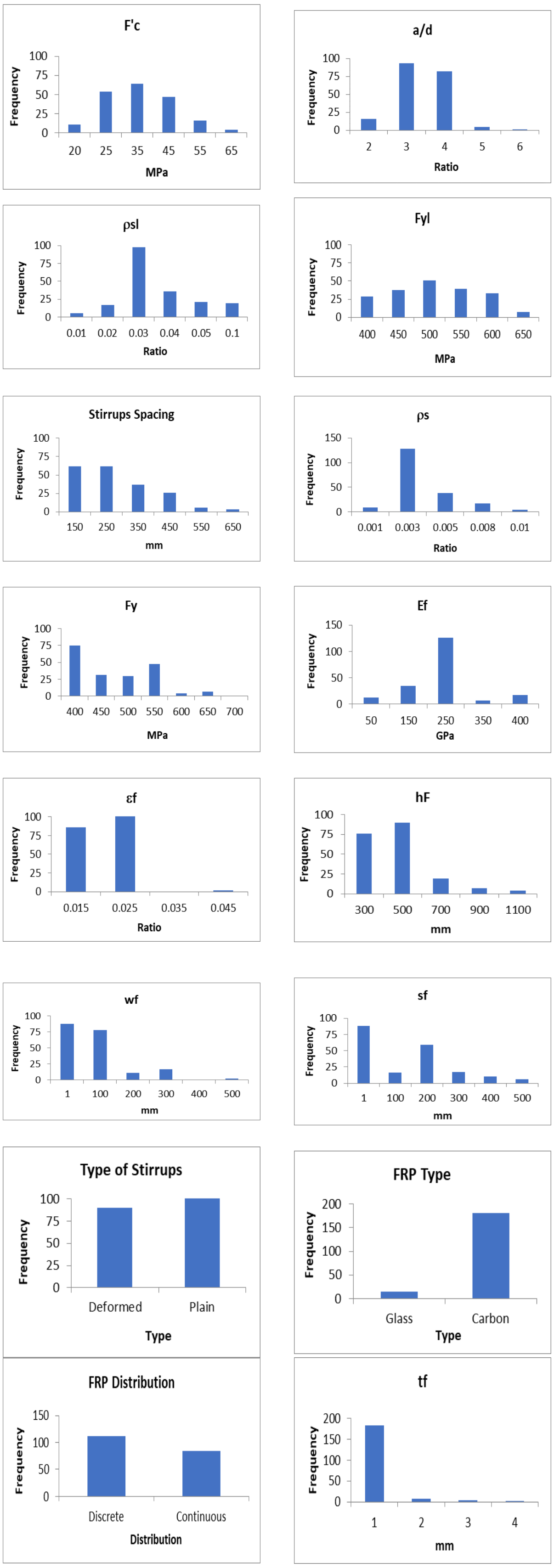

Fig. 2. Histogram of variables used for modeling

4. MODEL DEVELOPMENT

4.1 ANN Background

ANNs have been used in various fields (i.e., engineering, military, medical, biological, business, finance, manufacturing, etc.) to solve complicated problems by performing complex functions (Berrais, 1999; Jumaa and Yousif, 2018). ANNs perform simulated complex modeling and conduct calculations via training similar to the human brain. ANNs can be classified into two types according to their connectivity: feedforward and recurrent. Unlike the conventional numerical methods, ANNs feedforward do not provide closed-form solutions; however, it offers an accurate solution to a complex issue based on learning from a set of historical data called the training stage. In ANNs, the learning is obtained by adjusting the weights assigned to the connection iteratively to perform specific tasks. ANNs Learning is classified into three types: supervised, unsupervised, and reinforcement learning (Yao, 1999).

ANN is a group of small individually interconnected neurons (units) used to pass the information along interconnections. Each connection has an input value and a weight assigned to it, and the output will be a function of the summed value. ANNs can learn, respond, create the answer, and adjust their solution by learning from experience to meet the changing conditions. To enable that, the ANN needs to be trained first. ANNs learning, also called training, is performed by presenting a group of input units with a known output (target). In the learning process, the weights of the internal connections are adjusted by ANNs to minimize errors between the output provided by the network and the target output. This optimization algorithm is called backpropagation (Perera et al., 2014).

Data or input units used for learning can be empirical, theoretical, or a combination of both. Once the neural network training is completed, new patterns may be given to the network for prediction (testing stage). The training of ANNs neither requires complex mathematical equations nor computer models or impractical physical models. Indeed, the analysis by ANNs can be regarded as a background processing approach that the user does not need to know sophisticated mathematics (Perera et al., 2010).

Generally, the ANNs system consists of a fully interconnected input, an output layer, and many hidden layers (see Fig. 3). The values for the input layer come from the outside world then the output layer provides the predictions required. However, the hidden layer performs the main task that connects the input to the output layer and provides the network outcome by extracting and memorizing the main structures of the input trends. The ANNs are differentiated based on the activation function utilized by the hidden layers. The networks use two common activation functions: the sigmoid transfer function and the Gaussian radial basis function (Perera et al., 2010).

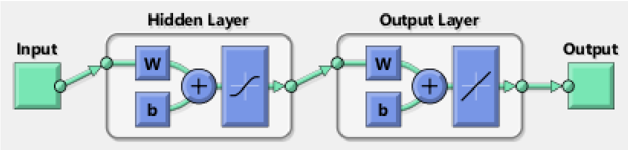

Fig. 3. ANN structure

4.2 ANN Modeling of EB-FRP Shear Strength (V_f)

This research study uses the feedforward two-layer network with sigmoid hidden neurons and linear output neurons for modeling. The training algorithm used to train the network is the most commonly used algorithm based on backpropagation Levenberg–Marquardt. MATLAB coding software was used to create, train, and implement the ANN modeling. The training of the network was performed iteratively to minimize the error between the network outputs and the target by considering the outcome of the mean square error (MSE) function, mean absolute error (MAE) function, and coefficient of determination (R^2). The neural network used in this study consisted of 16 inputs, one hidden layer, and one output layer. The number of neurons (nodes) in each layer depends on the number of variables in those nodes.

In the neural network configuration, the beam shear capacity was the target node (output) for the presented data set. Choosing the suitable input nodes from the list of parameters is critical in successfully implementing the system to optimize the ANN. On the other hand, there should be sufficient parameters and data points to represent the system properly. One should also remember that the higher number of input nodes in the neural network can also result in a less efficient training process. Considering the shear behavior of FRP strengthened beams, there are several critical parameters, some of which are also considered by existing design guidelines and are as follow: FRP configuration, FRP effective strain (ε_e), FRP elastic modulus (E_f), FRP reinforcement ratio (considering thickness, width, and spacing), inclination angles of the FRP layers, beam geometry, compressive strength of concrete (f_c'), shear span to depth ratio (a/d), transverse shear reinforcement properties (i.e., ratio, modulus, and yield strength), the ratio of longitudinal reinforcement, and its yield strength.

In the present study, it was decided to build the network considering 16 parameters. The sensitivity analysis of the model was performed only for the most influential parameters. As reported in the literature, the major parameters that significantly affect the shear behavior are: the FRP effective strain, FRP elastic modulus, FRP reinforcement ratio (ρ_f), FRP configuration (continuous or discrete), shear span to depth ratio (a/d), compressive strength of concrete (f_c'), the ratio of transverse shear (ρ_s) and its yield strength.

The 196 collected data points were randomly arranged into a training set (70%), a validating set (15%), and a testing set (15%). After conducting some trial runs, the number of hidden neurons chosen for training the networks was fixed at 15 neurons. The results of modeling using the commercial software called MATLAB is presented in Fig. 4.

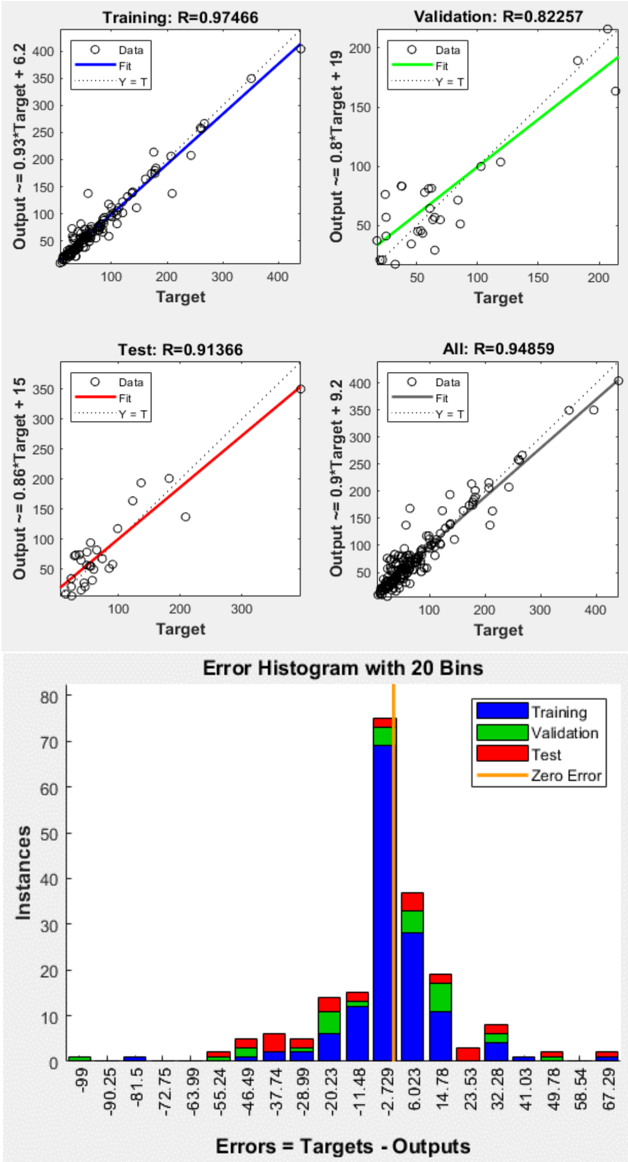

Fig. 4. Modeling error estimations from MATLAB

4.3 ANN Model versus Existing Conventional Models

The performance of the shear strength ANN prediction model is assessed by comparing the outputs with the actual experimental results (target) or the prediction of some existing design guidelines. The assessment was done based on the values of R^2, MSE, and MAE defined as follow:

$$\text{Correlation Coefficient (R)} = \Sigma\,[(X - Xm) \times (Y - Ym)] \,/\, \sqrt{[\Sigma\,(X - Xm)^2 \times \Sigma\,(Y - Ym)^2]} \quad (1)$$

$$R^2 = (\text{Correlation Coefficient}) \quad (2)$$

Where
X – Data points in Data set X, Y – Data points in Data set Y, Xm – Mean of Data set X, Ym – Mean of Data set Y

$$\text{MSE} = \frac{1}{n}\sum_{i=1}^{n}(exp - pred)^2 \quad (3)$$

$$\text{MAE} = \frac{1}{n}\sum_{i=1}^{n}|exp - pred| \quad (4)$$

The shear strength predictions by the ANN model for the testing data set (see Fig. 5a) and the set of all data points (see Fig. 5b) are plotted against the experimental results shown in Fig. 5. As can be inferred from the Fig., most data points fall near the diagonal line, also called the equality line. This indicates that the scatter is low around the equality line, suggesting how reasonable the shear strength prediction is by the ANN model presented in this paper.

The prediction comparison of the proposed ANN model to the predictions by the mostly used guidelines (namely ACI 440.2R and fib TG9.3) is plotted in Fig. 6. For a better comparison, statistical analysis is also conducted. The values in terms of MSE, MAE, R^2, the ratio between the experimental and predicted values ($V_{f,Pre}$ / $V_{f,exp}$), and the relative standard deviation also called coefficient of variation (CoV) are shown in Table 1. By comparing the values reported in Table 1 and observing Fig. 6, the more accurate predictions were obtained using the proposed ANN model.

5. SENSITIVITY ANALYSIS

Performing sensitivity analysis of the proposed model would be beneficial to determine the most critical parameters in modeling. Therefore, further analysis is conducted to assess the sensitivity of the network against different parameters. The sensitivity analysis is performed by varying one parameter at a time and keeping the rest of the parameters constant. Even though there exist a wide variety of parameters affecting the shear behavior of FRP strengthened beams, the sensitivity analysis in this study is focused only on eight major parameters: concrete compressive strength (f_c'), shear span to depth ratio (a/d), transverse shear reinforcement ratio (ρ_s), yield strength of shear reinforcement, distribution of EB-FRP layers (continuous or discrete), EB-FRP thickness (number of layers), and elastic modulus & ultimate strain of EB-FRP sheet.

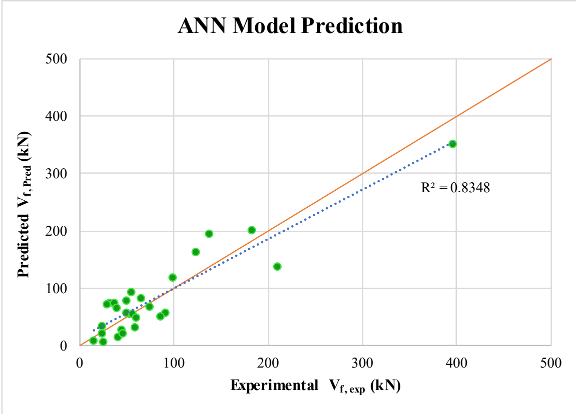

(a)

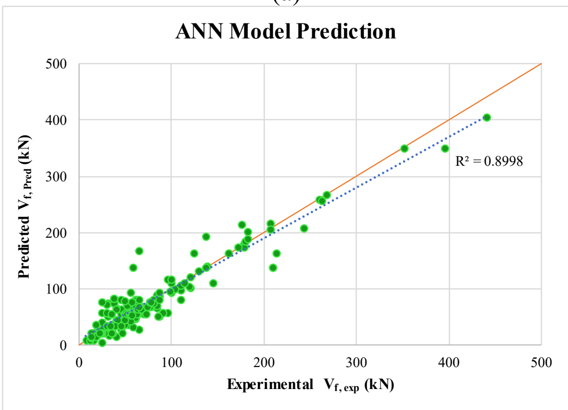

(b)

Fig. 5. ANN model prediction versus experimental result; a) testing data, b) all data

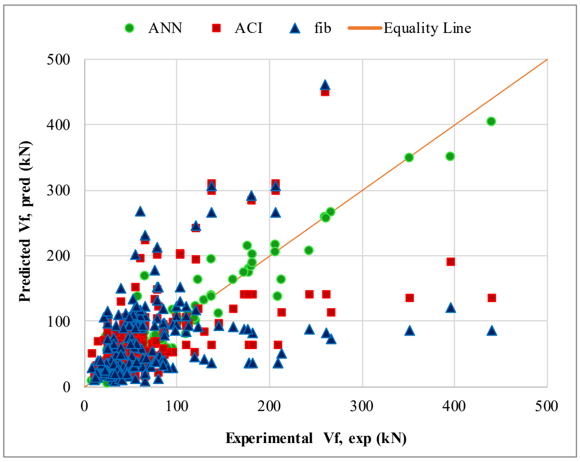

Fig. 6. Comparison of models prediction for V_f contribution to the shear strength

Table 1. Statistical comparison

Model	MSE		MAE		R^2		Vpre / Vexp		CoV	
	Test	All	Test	All	Test	All	Test	All	Test	All
ANN	960	430	26	13	0.83	0.90	1.14	1.11	0.38	0.52
ACI 440.2R	6617	5275	52	48	0.1	0.14	1.38	1.27	0.72	0.73
fib TG 9.3	4540	3670	44	40	0.29	0.31	1.47	1.35	0.66	0.63

The result of the sensitivity analysis is presented in Fig. 7. As can be seen in Fig. 7(a), by increasing the f_c', the V_f increases. This trend was expected since the higher compressive strength results in higher tensile strength and thus improves the bond between the interface of EB-FRP and concrete. Fig. 7(b) presents the a/d relationship with V_f. Given that if only slender beams are to be considered, the higher the a/d ratio is, the higher V_f capacity would be.

In Fig. 7(c), it can be observed that the shear strength predicted by the model decreases with the increase in "ρs". This behavior agrees with the previous research findings in the literature on the so-called adverse interaction between EB-FRP and steel stirrups (Chen et al., 2010; Mofidi and Chaallal, 2014; Ebead and Saeed, 2017; Li et al., 2018). The explanation can be that the higher the amount of shear reinforcement, the more distributed will be the cracking pattern which can trigger the premature debonding of EB-FRP. This results in a less effective contribution by EB-FRP. Furthermore, it is reported in the literature that the presence of EB-FRP disturbs the role of steel stirrups and may not reach yielding.

As illustrated in Fig. 7(d), the increase in "f_y" decreases the "V_f". A possible reason behind such observation is that in the presence of EB-FRP, if the steel is stronger (higher f_y) which will better arrest the cracks propagation thus will not trigger the full involvement of EB-FRP (Siddika et al., 2019). Because the EB-FRP gets fully activated once the steel is on the verge of yielding, this is another aspect of the adverse interaction which leads to a lower shear strength than expected.

Fig. 7(e) illustrates that the model predicts higher strength contribution when the EB-FRP sheet is applied in a continuous configuration compared to discrete strips. This is in agreement with the existing guidelines; however, this is controversial because some papers in the literature suggest that discrete configuration is superior to continuous. The model sensitivity is also investigated against the thickness of the EB-FRP layer (number of layers). It is clear from Fig. 7(f) that the strength gain is not proportional to the number of layers applied. This means that increasing the thickness (number of layers) does not increase the shear strength by the same ratio and, at some point, will become almost constant. In addition, providing a very thick layer of EB-FRP for shear strengthening will cause a brittle failure (Barakat et al., 2019), which can also be the interpretation of the sensitivity analysis showing a declining trend with an increase in EB-FRP thickness.

Fig. 7(g) shows that increase in moduli of EB-FRP results in less contribution to shear capacity. The possible explanation could be the brittleness of the system because higher modulus means more stiff behavior that can trigger a sudden debonding failure hence less effectiveness of EB-FRP strengthening. To some extent, a similar observation was made in a previous study (Bashir and Ashour, 2012) that higher E_f does not result in higher V_f values and remains constant at a certain degree. Referring to Fig. 7(h), it can be noticed that the prediction of V_f reduces with the increase in ultimate strain. This trend is attributed to the fact that GFRP sheets provide less shear strength despite having higher ultimate strain compared to CFRP sheets.

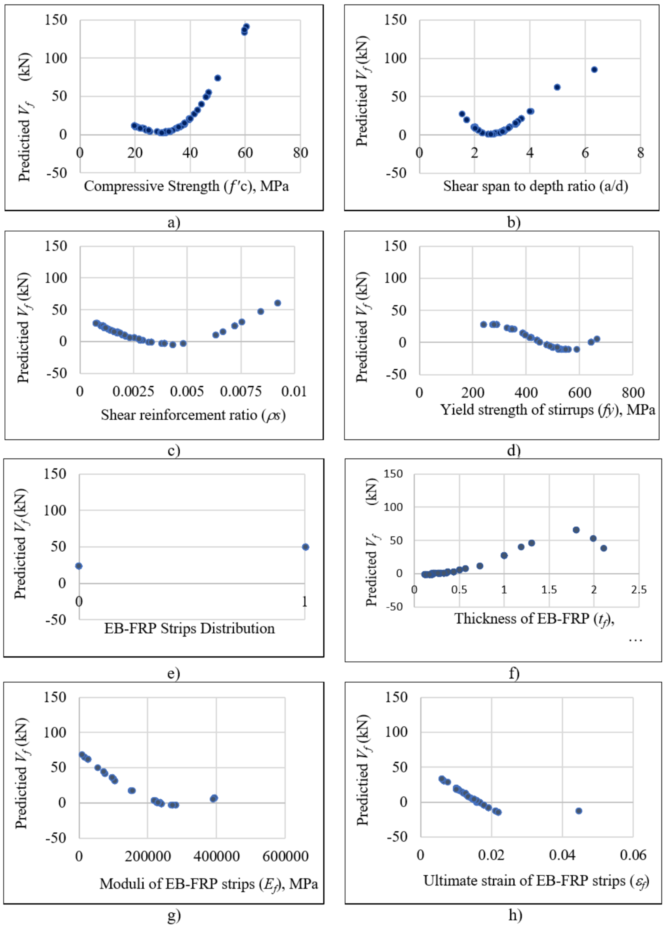

Fig. 7. Sensitivity analysis of ANN model

6. STANDALONE SOFTWARE APPLICATION

For ease in implementing the proposed ANN model, an executable program (app) is also developed in this study. The EXE program is made using an app design tool in MATLAB software, and its layout is shown in Fig. 8. To use the app the user just needs to input the material and member properties, and by clicking the solve button, the program will provide the shear strength contribution by EB-FRP (V_f). It is worth mentioning that the app works only for the beams with applied EB-FRP strengthening scheme.

7. SUMMARY AND CONCLUSIONS

This paper focused on developing a machine-learning (ML) model to predict the shear strength contribution (V_f) provided by externally bonded fiber-reinforced polymer (EB-FRP) to the shear capacity of strengthened RC beams. The study main objective is to model the contribution of EB-

FRP to the shear strength by considering the interaction between the steel stirrups and EB-FRP. In addition, the findings of this research will further contribute to the existing literature by illustrating the feasibility and capabilities of advanced machine learning models to solve complex behaviors as compared to conventional modeling techniques (linear and non-linear regression). A comprehensive database was built from existing literature (a total of 191 large-scale beams). The reported experimental database contains studies that performed experimental procedures representative of strengthening and rehabilitation/repair of beams having steel stirrups.

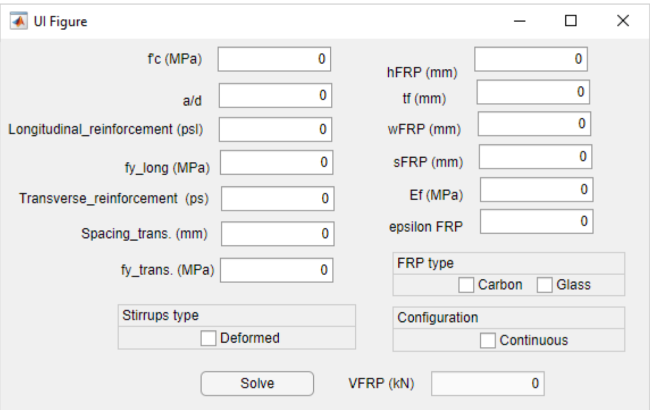

Fig. 8. App layout, built using MATLAB App design tool

ANN model was chosen as the primary ML model to be utilized in this research. The best-performed ANN model (i.e., one-hidden layer with 15 neurons in the hidden layer) was compared with other conventional EB-FRP strengthening models from the literature. The statistical results and graphical observation (data-scatter) indicate that the proposed ANN model is more accurate in its predictions. The MAE, MSE, and R^2 for the ANN model considering all the data points were found to be 13 kN, 430, and 0.9 respectively. While for the ACI & fib models the mentioned values were 48 kN & 40 kN, 5275 & 3670, and 0.14 & 0.31 respectively. The ANN model outperformed the conventional models, therefore suggesting the need to reconsider the current prediction practice of EB-FRP by simply adding the contribution of each component based on simple summation. The proposed model accounts for the interaction between steel stirrups and EB-FRP when predicting V_f without modifying the strength provided by the existing component of the member (Concrete and steel) as per the standard practice codes. A sensitivity analysis was conducted between some of the considered variables and the output (V_f). Overall, the effect of the considered parameters was analyzed and discussed. Finally, a standalone software application was built to host the best ANN model to facilitate the application of our proposed ANN model by other researchers and practitioners.

DATA AVAILABILITY

The database of the test specimens and the Matlab file along with the executable program can be shared upon request.

REFERENCES

ACI. 440.2R-17, 2017. American Concrete Institute.

Al-Rousan, R.Z., Issa A.M. 2016. The effect of beam depth on the shear behavior of reinforced concrete beams externally strengthened with carbon fiber–Reinforced polymer composites. Advances in Structural Engineering, 19, 1769–1779.

Altoubat, S., Karzad, A.S., Maalej, M., Barakat, S., Talha, M.J. 2020. Experimental study of the steel/CFRP interaction in shear-strengthened RC beams incorporating macro-synthetic fibers. Structures, 25, 88–98.

Altoubat, S., Karzad, A.S., Maalej, M. 2018. Strengthening of damaged reinforced concrete beams using externally bonded fiber reinforced polymer. Special Publication, 327, 28.

Baggio, D., Soudki, K., Noël, M. 2014. Strengthening of shear critical RC beams with various FRP systems. Construction and Building Materials, 66, 634–644.

Barakat, S., Al-Toubat, S., Leblouba, M., Burai, E.A. 2019. Behavioral trends of shear strengthened reinforced concrete beams with externally bonded fiber-reinforced polymer. Structural Engineering and Mechanics, 69, 579–589.

Bashir, R., Ashraf, A. 2012. Neural network modelling for shear strength of concrete members reinforced with FRP bars. Composites Part B: Engineering, 43, 3198–3207.

Berrais, A. 1999. Artificial neural networks in structural engineering: Concept and applications. Journal of King Abdulaziz University-Engineering Sciences, 12, 53–67.

Bousselham, A., Chaallal, O. 2006. Behavior of reinforced concrete t-beams strengthened in shear with carbon fiber-reinforced polymer - An experimental study. ACI Structural Journal. 103, 339–347.

Bukhari, I.A., Vollum, R.L., Ahmad, S, Sagaseta, J. 2010. Shear strengthening of reinforced concrete beams with CFRP. Magazine of Concrete Research, 9831, 65–77.

Chen, G.M., Teng, J.G., Chen, J.F., Rosenboom, O.A. 2010. Interaction between steel stirrups and shear-strengthening FRP strips in RC beams. Journal of Composites for Construction, 14, 498–509.

Chen, G.M., Zhang, Z., Li, Y.L., Li, X.Q., Zhou, C.Y. 2016. T-section RC beams shear-strengthened with anchored CFRP U-strips. Composite Structures, 144, 57–79.

Chen, J.F., Teng, J.G. 2003. Shear capacity of FRP-strengthened RC beams: FRP debonding. Construction and Building Materials 17, 27–41.

Ebead, U., Saeed, H. 2017. FRP/stirrups interaction of shear-strengthened beams. Materials and Structures, 50, 1–16.

Ekenel, M., John, J.M. 2007. Durability performance of RC beams strengthened with epoxy injection and CFRP fabrics. Construction and Building Materials, 21, 1182–1190.

El-Maaddawy, T., Chekfeh, Y. 2012. Retrofitting of severely shear-damaged concrete t-beams using externally bonded composites and mechanical end anchorage. Journal of Composites for Construction, 16, 693–704.

FIB. T.G.9.3., 2001. Externally Bonded FRP Reinforcement for RC Structures. International Federation for Structural Concrete (Fib). 14.

Alfarra, H., Maalej, M., Barakat, S. 2020. Shear strengthening of T-section RC beams using double-side externally bonded CFRP. In IOP Conference Series: Materials Science and Engineering, IOP Publishing, 829, 012021.

Hosseini, G. 2017. Capacity prediction of RC beams strengthened with FRP by artificial neural networks based on genetic algorithm. Journal of Soft Computing in Civil Engineering, 1, 93–98.

Jumaa, G.B., Yousif, A.R. 2018. Predicting shear capacity of FRP-reinforced concrete beams without stirrups by artificial neural networks, gene expression programming, and regression analysis. Advances in Civil Engineering.

Karzad, A.S., Leblouba, M., AlToubat, S., Maalej, M. 2019. Repair and strengthening of shear-deficient reinforced concrete beams using carbon fiber reinforced polymer. Composite Structures, 223.

Karzad, A.S., AlToubat S., Maalej M., Estephane, P. 2017. Repair of reinforced concrete beams using carbon fiber reinforced polymer. Matec Web of Conference, 120, 01008.

Li, W., Hu, C., Pan, Z., Peng, W., Yang, Y., Xing, F. 2018. A proposed strengthening model considering interaction of concrete-stirrup-FRP system for RC beams shear-strengthened with EB-FRP sheets. Journal of Reinforced Plastics and Composites, 37, 685–700.

Mofidi, A., Chaallal, O. 2014. Effect of steel stirrups on shear resistance gain due to externally bonded fiber-reinforced polymer strips and sheets. ACI Structural Journal, 111, 353–362.

Mofidi, A., Chaallal, O. 2011. Shear strengthening of RC beams with EB FRP: Influencing factors and conceptual debonding model. Journal of Composites for Construction, 15, 62–74.

Oller, E., Pujol, M., Marí, A. 2019. Contribution of externally bonded FRP shear reinforcement to the shear strength of RC beams. Composites Part B: Engineering, 164, 235–248.

Pellegrino, C., Modena, C. 2006. Fiber-reinforced polymer shear strengthening of reinforced concrete beams: Experimental study and analytical modeling. ACI Structural Journal, 103, 720–728.

Perera, R., Arteaga, A., Diego, A.D. 2010. Artificial intelligence techniques for prediction of the capacity of RC beams strengthened in shear with external FRP reinforcement. Composite Structures, 92, 1169–1175.

Perera, R., Tarazona, D., Ruiz, A., Martín, A. 2014. Application of artificial intelligence techniques to predict the performance of RC beams shear strengthened with NSM FRP rods. Formulation of Design Equations. Composites Part B: Engineering, 66, 162–173.

Sas, G. 2011. FRP shear strengthening of reinforced concrete beams, Ph.D. Dissertation, Lulea University of Technology, Lulea, Sweden.

Siddika, A, Al Mamun, M.A., Alyousef, R., Amran, Y.H.M. 2019. Strengthening of reinforced concrete beams by using fiber-reinforced polymer composites: A review. Journal of Building Engineering, 25, 100798.

Tanarslan, H.M., Secer, M., Kumanlioglu, A., 2012. An approach for estimating the capacity of RC beams strengthened in shear with FRP reinforcements using artificial neural networks. Construction and Building Materials, 30, 556–568.

Triantafillou, T., Costas, A., 2000. Design of concrete flexural members strengthened in shear with FRP. Journal of Composite for Construction ASCE, 4, 198–205.

Yao, X. 1999. Evolving artificial neural networks. Proceedings of the IEEE 87, 1423–1447.

APPENDIX

No	References	Specimens ID	Concrete strength	Beam dimension and properties								EB-FRP shear strengthening										
			fc (MPa)	bw (mm)	bf(T) (mm)	h (mm)	d (mm)	Cross Section	hfrp (mm)	Shear Span (a)	a/d	Type	Distri-bution	Wrapping Scheme	wf (mm)	Sf (mm)	Inclination β(°)	tf (mm)	Ef (MPa)	ff (MPa)	ε_f	ρf
1	(Pellegrino and Modena, 2002)	TR30D10	31.4	150	0	300	250	Rec	300	750	3.00	C	Ct	S	1	1	90	0.330	233600	4490	0.0192	0.0044
2	(Pellegrino and Modena, 2002)	TR30D2	31.4	150	0	300	250	Rec	300	750	3.00	C	Ct	S	1	1	90	0.500	233600	4490	0.0192	0.0067
3	(Pellegrino and Modena, 2002)	TR30D20	31.4	150	0	300	250	Rec	300	750	3.00	C	Ct	S	1	1	90	0.500	233600	4490	0.0192	0.0067
4	(Pellegrino and Modena, 2002)	TR30D4	31.4	150	0	300	250	Rec	300	750	3.00	C	Ct	S	1	1	90	0.330	233600	4490	0.0192	0.0044
5	(Pellegrino and Modena, 2002)	TR30D40	31.4	150	0	300	250	Rec	300	750	3.00	C	Ct	S	1	1	90	0.330	233600	4490	0.0192	0.0044
6	(Grande et al., 2009)	RS3Sa	21.0	250	0	450	428	Rec	450	1400	3.27	C	Ct	S	1	1	90	0.190	392000	2600	0.0066	0.0015
7	(Grande et al., 2009)	RS2Sa	21.0	250	0	450	428	Rec	450	1400	3.27	C	Ct	S	1	1	90	0.190	392000	2600	0.0066	0.0015
8	(Grande et al., 2009)	RS4Sb	21.0	250	0	450	428	Rec	450	1400	3.27	C	Ct	S	1	1	90	0.190	392000	2600	0.0066	0.0015
9	(Grande et al., 2009)	RS3Sb	21.0	250	0	450	428	Rec	450	1400	3.27	C	Ct	S	1	1	90	0.190	392000	2600	0.0066	0.0015
10	(Grande et al., 2013)	RS3SL3	21.0	250	0	450	380	Rec	450	1400	3.68	C	Ct	S	1	1	90	0.191	392000	2600	0.0066	0.0015
11	(Grande et al., 2013)	RS2SL3	21.0	250	0	450	380	Rec	450	1400	3.68	C	Ct	S	1	1	90	0.191	392000	2600	0.0066	0.0015
12	(Grande et al., 2013)	RS4SL3	21.0	250	0	450	380	Rec	450	1400	3.68	C	Ct	S	1	1	90	0.191	392000	2600	0.0066	0.0015
13	(Grande et al., 2013)	RS3SL3	21.0	250	0	450	380	Rec	450	1400	3.68	C	Ct	S	1	1	90	0.191	392000	2600	0.0066	0.0015
14	(Grande et al., 2013)	RS4SL4	21.0	250	0	450	380	Rec	450	1400	3.68	C	Ct	S	1	1	90	0.191	392000	2600	0.0066	0.0015
15	(Chaallal et al., 1998)	RS90a	35.0	150	0	250	215	Rec	250	600	2.79	C	Dt	S	50	100	90	1.000	150000	2400	0.0160	0.0067
16	(Chaallal et al., 1998)	RS90b	35.0	150	0	250	215	Rec	250	600	2.79	C	Dt	S	50	100	90	1.000	150000	2400	0.0160	0.0067
17	(Carolin and Taljsten, 2005)	B290	46.0	180	0	400	330	Rec	400	1000	3.03	C	Ct	S	1	1	90	0.110	234000	4500	0.0192	0.0012
18	(Carolin and Taljsten, 2005)	B390	46.0	180	0	400	330	Rec	400	1000	3.03	C	Ct	S	1	1	90	0.170	234000	4500	0.0192	0.0019
19	(Alsayed and Siddiqui, 2013)	BSV-1	35.0	200	0	300	265	Rec	300	750	2.83	C	Dt	S	50	150	90	1.000	77300	850	0.0110	0.0033
20	(Alsayed and Siddiqui, 2013)	BSI-2	35.0	200	0	300	265	Rec	300	750	2.83	C	Dt	S	50	150	30	1.000	77300	850	0.0110	0.0033
21	(Said Allam 2003)	S-1	32.0	120	0	200	175	Rec	200	450	2.57	C	Dt	S	50	100	90	0.260	230000	3500	0.0152	0.0022
22	(Said Allam 2003)	S-2	32.0	120	0	200	175	Rec	200	450	2.57	C	Dt	S	50	100	90	0.260	230000	3500	0.0152	0.0022
23	(Said Allam 2003)	S-3	32.0	120	0	200	175	Rec	200	450	2.57	C	Dt	S	50	100	90	0.260	230000	3500	0.0152	0.0022
24	(Said Allam 2003)	S-4	32.0	120	0	200	175	Rec	200	450	2.57	C	Dt	S	50	100	90	0.260	230000	3500	0.0152	0.0022
25	(Said Allam 2003)	W-3	32.0	120	0	200	175	Rec	200	450	2.57	C	Ct	S	1	1	90	0.260	230000	3500	0.0152	0.0043
26	(Said Allam 2003)	W-4	32.0	120	0	200	175	Rec	200	450	2.57	C	Ct	S	1	1	90	0.260	230000	3500	0.0152	0.0043

No	References	Specimens ID	Longitudinal Reinforcement				Steel stirrups							Test results				
			Esl (Mpa)	fyl (Mpa)	Asl (mm2)	ρsl	Type	Diameter (mm)	Spacing (mm)	Es (MPa)	fy (MPa)	As (mm2)	ρs	Vu, test	Mode of Failure	Vf, test	Vc+Vs, test	Vf gain %
1	(Pellegrino and Modena, 2002)	TR30D10	210000	548	NA	0.0044	Deformed	8	200	210000	548	100.53	0.0034	193.0	DB	31.5	161.5	19.5
2	(Pellegrino and Modena, 2002)	TR30D2	210000	548	NA	0.0066	Deformed	8	200	210000	548	100.53	0.0034	213.3	DB	51.8	161.5	32.1
3	(Pellegrino and Modena, 2002)	TR30D20	210000	548	NA	0.0066	Deformed	8	200	210000	548	100.53	0.0034	247.5	DB	86	161.5	53.3
4	(Pellegrino and Modena, 2002)	TR30D4	210000	548	NA	0.0044	Deformed	8	200	210000	548	100.53	0.0034	208.8	DB	47.3	161.5	29.3
5	(Pellegrino and Modena, 2002)	TR30D40	210000	548	NA	0.0044	Deformed	8	200	210000	548	100.53	0.0034	212.0	DB	50.5	161.5	31.3
6	(Grande et al., 2009)	RS3Sa	210000	476	2148.8	0.0201	Deformed	8	300	210000	476	100.53	0.0013	205.0	DB	45	160	28.1
7	(Grande et al., 2009)	RS2Sa	210000	476	2148.8	0.0201	Deformed	8	200	210000	476	100.53	0.0020	240.0	DB	25	215	11.6
8	(Grande et al., 2009)	RS4Sb	210000	476	2148.8	0.0201	Deformed	8	400	210000	476	100.53	0.0010	180.0	DB	55	125	44.0
9	(Grande et al., 2009)	RS3Sb	210000	476	2148.8	0.0201	Deformed	8	300	210000	476	100.53	0.0013	220.0	DB	60	160	37.5
10	(Grande et al., 2013)	RS3SL3	210000	476	2148.8	0.0226	Deformed	8	300	210000	476	100.53	0.0013	205.0	DB	45	160	28.1
11	(Grande et al., 2013)	RS2SL3	210000	476	2148.8	0.0226	Deformed	8	200	210000	476	100.53	0.0020	240.0	DB	25	215	11.6
12	(Grande et al., 2013)	RS4SL3	210000	476	2148.8	0.0226	Deformed	8	400	210000	476	100.53	0.0010	180.0	DB	55	125	44.0
13	(Grande et al., 2013)	RS3SL3	210000	476	2148.8	0.0226	Deformed	8	300	210000	476	100.53	0.0013	220.0	DB	60	160	37.5
14	(Grande et al., 2013)	RS4SL4	210000	476	2148.8	0.0226	Deformed	8	400	210000	476	100.53	0.0010	185.0	DB	45	140	32.1
15	(Chaallal et al., 1998)	RS90a	200000	400	530.0	0.0160	Plain	6	200	200000	400	56.55	0.0019	87.5	DB	34.2	53.3	64.2
16	(Chaallal et al., 1998)	RS90b	200000	400	530.0	0.0160	Plain	6	200	200000	400	56.55	0.0019	95.0	DB	41.7	53.3	78.2
17	(Carolin and Taljsten, 2005)	B290	210000	515	2413.0	0.0410	Plain	6	200	210000	515	56.55	0.0016	298.0	DB	61	237	25.7
18	(Carolin and Taljsten, 2005)	B390	210000	515	2413.0	0.0410	Plain	6	200	210000	515	56.55	0.0016	298.0	DB	61	237	25.7
19	(Alsayed and Siddiqui, 2013)	BSV-1	200000	480	942.5	0.0178	Plain	6	150	200000	275	56.55	0.0019	48.2	DB	7.6	40.6	18.7
20	(Alsayed and Siddiqui, 2013)	BSI-2	200000	480	942.5	0.0178	Plain	6	150	200000	275	56.55	0.0019	55.4	DB	14.8	40.6	36.5
21	(Said Allam 2003)	S-1	200000	400	603.2	0.0287	Plain	6	120	200000	280	56.55	0.0039	100.0	DB	20.0	80	25.0
22	(Said Allam 2003)	S-2	200000	400	603.2	0.0287	Plain	6	120	200000	280	56.55	0.0039	82.5	DB	20.0	62.5	32.0
23	(Said Allam 2003)	S-3	200000	400	603.2	0.0287	Plain	6	120	200000	280	56.55	0.0039	78.7	DB	16.2	62.5	25.9
24	(Said Allam 2003)	S-4	200000	400	603.2	0.0287	Plain	6	120	200000	280	56.55	0.0039	76.2	DB	13.7	62.5	21.9
25	(Said Allam 2003)	W-3	200000	400	603.2	0.0287	Plain	6	120	200000	280	56.55	0.0039	87.5	DB	25.0	62.5	40.0
26	(Said Allam 2003)	W-4	200000	400	603.2	0.0287	Plain	6	120	200000	280	56.55	0.0039	86.2	DB	23.7	62.5	37.9

No	References	Specimens ID	Concrete strength	Beam dimension and properties								EB-FRP shear strengthening										
			fc (MPa)	bw (mm)	bf(T) (mm)	h (mm)	d (mm)	Cross Section	hfrp (mm)	Shear Span (a)	a/d	Type	Distri-bution	Wrapping Scheme	wf (mm)	Sf (mm)	Inclination β(°)	tf (mm)	Ef (MPa)	ff (MPa)	ε_f	ρf
27	(Sato et al., 1997)	No.2	36.3	150	400	300	240	T	200	600	2.50	C	Ct	U	1	1	90	0.110	230000	3480	0.0151	0.0015
28	(Sato et al., 1997)	No.3	35.8	150	400	300	240	T	200	600	2.50	C	Ct	U	1	1	90	0.110	230000	3480	0.0151	0.0015
29	(Chaallal et al., 2002)	G5.5-1L	37.9	122	584	445	343	T	356	686	2.00	C	Ct	U	1	1	90	0.150	231000	3650	0.0158	0.0025
30	(Chaallal et al., 2002)	G5.5-2L	37.9	122	584	445	343	T	356	686	2.00	C	Ct	U	1	1	90	0.290	231000	3650	0.0158	0.0048
31	(Chaallal et al., 2002)	G8.0-1L	37.9	122	584	445	343	T	356	686	2.00	C	Ct	U	1	1	90	0.150	231000	3650	0.0158	0.0025
32	(Chaallal et al., 2002)	G8.0-2L	37.9	122	584	445	343	T	356	686	2.00	C	Ct	U	1	1	90	0.290	231000	3650	0.0158	0.0048
33	(Chaallal et al., 2002)	G8.0-3L	37.9	122	584	445	343	T	356	686	2.00	C	Ct	U	1	1	90	0.440	231000	3650	0.0158	0.0072
34	(Chaallal et al., 2002)	G16-1L	37.9	122	584	445	343	T	356	686	2.00	C	Ct	U	1	1	90	0.150	231000	3650	0.0158	0.0025
35	(Chaallal et al., 2002)	G16-2L	37.9	122	584	445	343	T	356	686	2.00	C	Ct	U	1	1	90	0.290	231000	3650	0.0158	0.0048
36	(Chaallal et al., 2002)	G24-1L	37.9	122	584	445	343	T	356	686	2.00	C	Ct	U	1	1	90	0.150	231000	3650	0.0158	0.0025
37	(Chaallal et al., 2002)	G24-2L	37.9	122	584	445	343	T	356	686	2.00	C	Ct	U	1	1	90	0.290	231000	3650	0.0158	0.0048
38	(Chaallal et al., 2002)	G24-3L	37.9	122	584	445	343	T	356	686	2.00	C	Ct	U	1	1	90	0.440	231000	3650	0.0158	0.0072
39	(Khalifa and Naani 2002)	SW3-2	20.0	150	0	305	255	Rec	305	760	2.98	C	Dt	U	1	1	90	0.170	228000	3790	0.0166	0.0023
40	(Khalifa and Naani 2002)	SW4-2	20.0	150	0	305	255	Rec	305	1025	4.02	C	Dt	U	1	1	90	0.170	228000	3790	0.0166	0.0023
41	(Pellegrino and Modena, 2006)	A-U1-C-17	41.4	150	0	300	250	Rec	300	750	3.00	C	Ct	U	1	1	90	0.170	230000	3450	0.0150	0.0023
42	(Pellegrino and Modena, 2006)	A-U1-C-20	41.4	150	0	300	250	Rec	300	750	3.00	C	Ct	U	1	1	90	0.170	230000	3450	0.0150	0.0023
43	(Pellegrino and Modena, 2006)	A-U1-S-17	41.4	150	0	300	250	Rec	300	750	3.00	C	Ct	U	1	1	90	0.170	230000	3450	0.0150	0.0023
44	(Pellegrino and Modena, 2006)	A-U1-S-20	41.4	150	0	300	250	Rec	300	750	3.00	C	Ct	U	1	1	90	0.170	230000	3450	0.0150	0.0023
45	(Pellegrino and Modena, 2006)	A-U2-C-17	41.4	150	0	300	250	Rec	300	750	3.00	C	Ct	U	1	1	90	0.330	230000	3450	0.0150	0.0044
46	(Pellegrino and Modena, 2006)	A-U2-C-20	41.4	150	0	300	250	Rec	300	750	3.00	C	Ct	U	1	1	90	0.330	230000	3450	0.0150	0.0044
47	(Pellegrino and Modena, 2006)	A-U2-S-17	41.4	150	0	300	250	Rec	300	750	3.00	C	Ct	U	1	1	90	0.330	230000	3450	0.0150	0.0044
48	(Pellegrino and Modena, 2008)	TrBU1-1	46.2	150	0	300	242	Rec	300	750	3.10	C	Dt	U	500	500	90	0.165	230000	3450	0.0150	0.0022
49	(Pellegrino and Modena, 2008)	TrBU2-1	46.2	150	0	300	242	Rec	300	750	3.10	C	Dt	U	500	500	90	0.330	230000	3450	0.0150	0.0044
50	(Grande et al., 2009)	RS3Ua	21.0	250	0	450	428	Rec	450	1400	3.27	C	Ct	U	1	1	90	0.190	392000	2600	0.0066	0.0015
51	(Grande et al., 2009)	RS2Ua	21.0	250	0	450	428	Rec	450	1400	3.27	C	Ct	U	1	1	90	0.190	392000	2600	0.0066	0.0015
52	(Grande et al., 2009)	RS4Ub	21.0	250	0	450	428	Rec	450	1400	3.27	C	Ct	U	1	1	90	0.190	392000	2600	0.0066	0.0015
53	(Kim, 2011)	24-3-1r+	20.5	355	711	610	520	T	508	1600	3.08	C	Dt	U+	127	254	90	0.280	102042	1062	0.0104	0.0008
54	(Kim, 2011)	24-3,3+	20.5	355	711	610	520	T	508	1600	3.08	C	Dt	U+	127	254	90	0.280	102042	1062	0.0104	0.0008
55	(Kim, 2011)	24-3,4+	20.5	355	711	610	520	T	508	1600	3.08	C	Dt	U+	127	254	90	0.280	102042	1062	0.0104	0.0008
56	(Kim, 2011)	24-3,5+	20.5	355	711	610	520	T	508	1600	3.08	C	Dt	U+	127	254	90	0.500	56537	724	0.0128	0.0014
57	(Kim, 2011)	24-3,6+	20.5	355	711	610	520	T	508	1600	3.08	C	Dt	U+	127	254	90	0.165	227527	3729	0.0164	0.0005
58	(Kim, 2011)	24-3,7+	20.5	355	711	610	520	T	508	1600	3.08	C	Ct	U+	1	1	90	0.280	102042	1062	0.0104	0.0016
59	(Kim, 2011)	24-3,8+	20.5	355	711	610	520	T	508	1600	3.08	C	Dt	U+	127	254	90	0.560	102043	1063	0.0104	0.0016
60	(Kim, 2011)	24-3,10+	20.5	355	711	610	520	T	508	1100	2.12	C	Dt	U+	127	254	90	0.280	102045	1065	0.0104	0.0008
61	(Kim, 2011)	24-2.1-1+	20.5	355	711	610	520	T	508	800	1.54	C	Dt	U+	127	254	90	0.280	102046	1066	0.0104	0.0008
62	(Kim, 2011)	24-1.5-4+	20.5	355	711	610	520	T	508	3300	6.35	C	Dt	U+	127	254	90	0.280	102049	1069	0.0105	0.0008
63	(Kim, 2011)	48-3-2+	20.5	355	533	1220	1092	T	1017	3300	3.02	C	Dt	U+	254	508	90	0.280	102050	1070	0.0105	0.0008
64	(Kim, 2011)	48-3-4+	20.5	355	533	1220	1092	T	1017	3300	3.02	C	Dt	U+	254	508	45	0.280	102052	1072	0.0105	0.0008
65	(Kim, 2011)	48-3-6r+	20.5	355	533	1220	1092	T	1017	3300	3.02	C	Dt	U+	254	508	90	0.280	102053	1073	0.0105	0.0008
66	(Kim, 2011)	48-3-8+	20.5	355	533	1220	1092	T	1017	3300	3.02	C	Dt	U+	254	508	90	0.560	102056	1076	0.0105	0.0016
67	(Colalillo, 2012)	MC-S5-US	41.4	400	0	650	545	Rec	610	1675	3.07	C	Dt	U	100	200	90	1.000	95804	990	0.0103	0.0025
68	(Colalillo, 2012)	MC-S5-UA	42.8	400	0	650	545	Rec	610	1675	3.07	C	Ct	U	1	1	90	1.000	95805	991	0.0103	0.0050
69	(Colalillo, 2012)	MC-S2-US	42.8	400	0	650	545	Rec	610	1675	3.07	C	Dt	U	100	200	90	1.000	95808	994	0.0104	0.0025
70	(Colalillo, 2012)	MC-S2-UA	42.8	400	0	650	545	Rec	610	1675	3.07	C	Ct	U	1	1	90	1.000	95809	995	0.0104	0.0050

No	References	Specimens ID	Longitudinal Reinforcement				Steel stirrups							Test results				
			Esl (Mpa)	fyl (Mpa)	Asl (mm2)	ρsl	Type	Diameter (mm)	Spacing (mm)	Es (MPa)	fy (MPa)	As (mm2)	ρs	Vu, test	Mode of Failure	Vf, test	Vc+Vs, test	Vf gain %
27	(Sato et al., 1997)	No.2	192000	396	1963.0	0.0550	Deformed	8	100	187000	386	100.53	0.0067	264.0	DB	65	199	32.7
28	(Sato et al., 1997)	No.3	192000	396	1963.0	0.0550	Deformed	8	100	187000	386	100.53	0.0067	223.0	DB	24	199	12.1
29	(Chaallal et al., 2002)	G5.5-1L	203000	441	1134.0	0.0270	Deformed	10	140	203000	441	157.08	0.0092	320.3	RT	31.2	289.1	10.8
30	(Chaallal et al., 2002)	G5.5-2L	203000	441	1134.0	0.0270	Deformed	10	140	203000	441	157.08	0.0092	342.5	RT	53.4	289.1	18.5
31	(Chaallal et al., 2002)	G8.0-1L	203000	441	1134.0	0.0270	Deformed	10	203	203000	441	157.08	0.0063	298.0	RT	31.1	266.9	11.7
32	(Chaallal et al., 2002)	G8.0-2L	203000	441	1134.0	0.0270	Deformed	10	203	203000	441	157.08	0.0063	329.2	RT	62.3	266.9	23.3
33	(Chaallal et al., 2002)	G8.0-3L	203000	441	1134.0	0.0270	Deformed	10	203	203000	441	157.08	0.0063	351.4	RT	84.5	266.9	31.7
34	(Chaallal et al., 2002)	G16-1L	203000	441	1134.0	0.0270	Deformed	10	406	203000	441	157.08	0.0032	275.8	RT	40	235.8	17.0
35	(Chaallal et al., 2002)	G16-2L	203000	441	1134.0	0.0270	Deformed	10	406	203000	441	157.08	0.0032	320.3	RT	84.5	235.8	35.8
36	(Chaallal et al., 2002)	G24-1L	203000	441	1134.0	0.0270	Deformed	10	610	203000	441	157.08	0.0021	258.0	RT	53.4	204.6	26.1
37	(Chaallal et al., 2002)	G24-2L	203000	441	1134.0	0.0270	Deformed	10	610	203000	441	157.08	0.0021	253.5	RT	48.9	204.6	23.9
38	(Chaallal et al., 2002)	G24-3L	203000	441	1134.0	0.0270	Deformed	10	610	203000	441	157.08	0.0021	258.0	RT	53.4	204.6	26.1
39	(Khalifa and Naani 2002)	SW3-2	200000	460	1608.0	0.0420	Deformed	10	125	200000	350	157.0796	0.0084	177.0	DB	51	126	40.5
40	(Khalifa and Naani 2002)	SW4-2	200000	460	1608.0	0.0420	Deformed	10	125	200000	350	157.0796	0.0084	180.0	DB	81	99	81.8
41	(Pellegrino and Modena, 2006)	A-U1-C-17	200000	534	2827.0	0.0750	Deformed	8	170	200000	534	100.53	0.0039	238.1	DB	52.9	185.2	28.6
42	(Pellegrino and Modena, 2006)	A-U1-C-20	200000	534	2827.0	0.0750	Deformed	8	200	200000	534	100.53	0.0034	225.0	DB	55.8	169.2	33.0
43	(Pellegrino and Modena, 2006)	A-U1-S-17	200000	534	2827.0	0.0750	Deformed	8	170	200000	534	100.53	0.0039	247.3	DB	49.2	198.1	24.8
44	(Pellegrino and Modena, 2006)	A-U1-S-20	200000	534	2827.0	0.0750	Deformed	8	200	200000	534	100.53	0.0034	235.1	DB	31.6	203.5	15.5
45	(Pellegrino and Modena, 2006)	A-U2-C-17	200000	534	2827.0	0.0750	Deformed	8	170	200000	534	100.53	0.0039	243.0	DB	57.8	185.2	31.2
46	(Pellegrino and Modena, 2006)	A-U2-C-20	200000	534	2827.0	0.0750	Deformed	8	200	200000	534	100.53	0.0034	229.7	DB	60.5	169.2	35.8
47	(Pellegrino and Modena, 2006)	A-U2-S-17	200000	534	2827.0	0.0750	Deformed	8	170	200000	534	100.53	0.0039	218.9	DB	20.8	198.1	10.5
48	(Pellegrino and Modena, 2008)	TrBU1-1	206000	534	2827.4	0.0779	Deformed	8	140	206000	534	100.53	0.0048	252.9	DB	24.4	228.5	10.7
49	(Pellegrino and Modena, 2008)	TrBU2-1	206000	534	2827.4	0.0779	Deformed	8	140	206000	534	100.53	0.0048	264.8	DB	36.3	228.5	15.9
50	(Grande et al., 2009)	RS3Ua	210000	476	2148.8	0.0201	Deformed	8	300	210000	476	100.53	0.0013	270.0	RT	110	160	68.8
51	(Grande et al., 2009)	RS2Ua	210000	476	2148.8	0.0201	Deformed	8	200	210000	476	100.53	0.0020	280.0	RT	65	215	30.2
52	(Grande et al., 2009)	RS4Ub	210000	476	2148.8	0.0201	Deformed	8	400	210000	476	100.53	0.0010	225.0	RT	100	125	80.0
53	(Kim, 2011)	24-3-1r+	200000	554	6605.2	0.0358	Deformed	10	254	200000	420	157.08	0.0017	676.1	RT	209.1	467	44.8
54	(Kim, 2011)	24-3,3+	200000	554	6605.2	0.0358	Deformed	10	254	200000	420	157.08	0.0017	524.9	RT	57.9	467	12.4
55	(Kim, 2011)	24-3,4+	200000	554	6605.2	0.0358	Deformed	10	254	200000	420	157.08	0.0017	676.1	RT	209.1	467	44.8
56	(Kim, 2011)	24-3,5+	200000	554	6605.2	0.0358	Deformed	10	254	200000	420	157.08	0.0017	645.0	RT	178	467	38.1
57	(Kim, 2011)	24-3,6+	200000	554	6605.2	0.0358	Deformed	10	254	200000	420	157.08	0.0017	596.0	RT	129	467	27.6
58	(Kim, 2011)	24-3,7+	200000	554	6605.2	0.0358	Deformed	10	254	200000	420	157.08	0.0017	733.9	RT	266.9	467	57.2
59	(Kim, 2011)	24-3,8+	200000	554	6605.2	0.0358	Deformed	10	254	200000	420	157.08	0.0017	680.5	RT	213.5	467	45.7
60	(Kim, 2011)	24-3,10+	200000	554	6605.2	0.0358	Deformed	10	254	200000	420	157.08	0.0017	645.0	RT	178	467	38.1
61	(Kim, 2011)	24-2.1-1+	200000	554	6605.2	0.0358	Deformed	10	254	200000	420	157.08	0.0017	756.2	RT	182.4	573.8	31.8
62	(Kim, 2011)	24-1.5-4+	200000	554	6605.2	0.0358	Deformed	10	102	200000	420	157.08	0.0043	1174.3	RT	137.9	1036.4	13.3
63	(Kim, 2011)	48-3-2+	200000	554	9651.0	0.0249	Deformed	10	457	200000	420	157.08	0.0010	1005.2	RT	351.3	653.9	53.7
64	(Kim, 2011)	48-3-4+	200000	554	9651.0	0.0249	Deformed	10	457	200000	420	157.08	0.0010	1049.7	RT	395.8	653.9	60.5
65	(Kim, 2011)	48-3-6r+	200000	554	9651.0	0.0249	Deformed	10	102	200000	420	157.08	0.0043	1454.5	RT	440.4	1014.1	43.4
66	(Kim, 2011)	48-3-8+	200000	554	9651.0	0.0249	Deformed	10	102	200000	420	157.08	0.0043	1134.2	RT	120.1	1014.1	11.8
67	(Colalillo, 2012)	MC-S5-US	213600	481	5654.9	0.0259	Deformed	10	500	194900	501	157.08	0.0008	518.0	DB	103	415	24.8
68	(Colalillo, 2012)	MC-S5-UA	213600	481	5654.9	0.0259	Deformed	10	500	194900	501	157.08	0.0008	622.0	DB	207	415	49.9
69	(Colalillo, 2012)	MC-S2-US	213600	481	5654.9	0.0259	Deformed	10	250	194900	501	157.08	0.0016	629.0	DB	78	551	14.2
70	(Colalillo, 2012)	MC-S2-UA	213600	481	5654.9	0.0259	Deformed	10	250	194900	501	157.08	0.0016	688.0	DB	137	551	24.9

No	References	Specimens ID	Concrete strength	Beam dimension and properties								EB-FRP shear strengthening										
			fc (MPa)	bw (mm)	bf(T) (mm)	h (mm)	d (mm)	Cross Section	hfrp (mm)	Shear Span (a)	a/d	Type	Distri-bution	Wrapping Scheme	wf (mm)	Sf (mm)	Inclination β(°)	tf (mm)	Ef (MPa)	ff (MPa)	ε_f	ρf
71	(Grande et al., 2013)	RS3UL3	21.0	250	0	450	380	Rec	450	1140	3.00	C	Ct	U	1	1	90	0.191	392000	2600	0.0066	0.0015
72	(Grande et al., 2013)	RS2UL3	21.0	250	0	450	380	Rec	450	1140	3.00	C	Ct	U	1	1	90	0.191	392000	2600	0.0066	0.0015
73	(Grande et al., 2013)	RS4UL3	21.0	250	0	450	380	Rec	450	1140	3.00	C	Ct	U	1	1	90	0.191	392000	2600	0.0066	0.0015
74	(Grande et al., 2013)	RS4UL4	21.0	250	0	450	380	Rec	450	1520	4.00	C	Ct	U	1	1	90	0.191	392000	2600	0.0066	0.0015
75	(Koutas and Triantafillou, 2013)	U2C	22.7	140	300	300	262	T	220	600	2.29	C	Ct	U	1	1	90	0.230	230000	3790	0.0165	0.0033
76	(Koutas and Triantafillou, 2013)	U2C-AN3Ch+	22.3	140	300	300	262	T	220	600	2.29	C	Ct	U+	1	1	90	0.230	230000	3791	0.0165	0.0033
77	(Koutas and Triantafillou, 2013)	U2C-AN3Cin+	22.2	140	300	300	262	T	220	600	2.29	C	Ct	U+	1	1	90	0.230	230000	3792	0.0165	0.0033
78	(Koutas and Triantafillou, 2013)	U2C-AN5Cin+	22.9	140	300	300	262	T	220	600	2.29	C	Ct	U+	1	1	90	0.230	230000	3793	0.0165	0.0033
79	(Koutas and Triantafillou, 2013)	U2G-AN3Gin+	22.9	140	300	300	262	T	220	600	2.29	G	Ct	U+	1	1	90	0.720	72400	3240	0.0448	0.0103
80	(Azate et al 2013)	U90C5	25.0	250	0	420	355	Rec	420	1260	3.55	C	Ct	U	1	1	90	0.293	240000	4000	0.0167	0.0023
81	(Azate et al 2013)	U90C5	23.0	250	0	420	355	Rec	420	1260	3.55	C	Ct	U	1	1	90	0.293	240000	4000	0.0167	0.0023
82	(Azate et al 2013)	U90S5	37.0	250	0	420	355	Rec	420	1260	3.55	C	Dt	U	300	200	90	0.293	240000	4000	0.0167	0.0035
83	(Azate et al 2013)	U90S5	28.0	250	0	420	355	Rec	420	1260	3.55	C	Dt	U	300	200	90	0.293	240000	4000	0.0167	0.0035
84	(Azate et al 2013)	U90C3	30.0	250	0	420	355	Rec	420	1260	3.55	C	Ct	U	1	1	90	0.165	240000	3800	0.0158	0.0013
85	(Azate et al 2013)	U90C3	30.0	250	0	420	355	Rec	420	1260	3.55	C	Ct	U	1	1	90	0.165	240000	3800	0.0158	0.0013
86	(Azate et al 2013)	U90S3	20.0	250	0	420	355	Rec	420	1260	3.55	C	Dt	U	300	200	90	0.165	240000	3800	0.0158	0.0020
87	(Azate et al 2013)	U90S3	23.0	250	0	420	355	Rec	420	1260	3.55	C	Dt	U	300	200	90	0.165	240000	3800	0.0158	0.0020
88	(Azate et al 2013)	U90S3	28.0	250	0	420	355	Rec	420	1260	3.55	C	Dt	U	300	200	90	0.165	240000	3800	0.0158	0.0020
89	(Azate et al 2013)	U45S5	31.0	250	0	420	355	Rec	420	1260	3.55	C	Dt	U	300	200	45	0.293	240000	4000	0.0167	0.0035
90	(Azate et al 2013)	U45S3	20.0	250	0	420	355	Rec	420	1260	3.55	C	Dt	U	300	200	45	0.165	240000	3800	0.0158	0.0020
91	(Azate et al 2013)	U45S3	31.0	250	0	420	355	Rec	420	1260	3.55	C	Dt	U	300	200	45	0.165	240000	3800	0.0158	0.0020
92	(Shamim Sheikh 2014)	S5-US	47.0	400	0	650	545	Rec	650	1675	3.07	C	Dt	U	100	200	90	1.000	95300	961	0.0101	0.0025
93	(Shamim Sheikh 2014)	S5-UA	47.0	400	0	650	545	Rec	650	1675	3.07	C	Dt	U	1	1	90	1.000	95300	961	0.0101	0.0050
94	(Shamim Sheikh 2014)	S2-US	47.0	400	0	650	545	Rec	650	1675	3.07	C	Dt	U	100	200	90	1.000	95300	961	0.0101	0.0025
95	(Shamim Sheikh 2014)	S2-UA	47.0	400	0	650	545	Rec	650	1675	3.07	C	Dt	U	1	1	90	1.000	95300	961	0.0101	0.0050
96	(Karzad, 2015)	SU-SS-2L-36	36.4	230	0	390	330	Rec	390	1150	3.48	C	Dt	U	100	150	90	0.332	230000	4900	0.0213	0.0019
97	(Karzad, 2015)	SU-SS-2L-36	36.4	230	0	390	330	Rec	390	1150	3.48	C	Dt	U	100	150	90	0.332	230000	4900	0.0213	0.0019
98	(Long and Marian, 2015)	G1-GFRP3	31.2	300	0	600	525	Rec	600	895	1.70	G	Ct	U	1	1	90	3.900	26100	575	0.0220	0.0260
99	(Long and Marian, 2015)	G2-GFRP-2A	29.4	200	0	500	442	Rec	500	880	1.99	G	Ct	U	1	1	90	2.600	26100	575	0.0220	0.0260
100	(Long and Marian, 2015)	G2-CFRP-2	29.4	200	0	500	442	Rec	500	880	1.99	C	Ct	U	1	1	90	2.000	95800	986	0.0103	0.0200
101	(Long and Marian, 2015)	G2-GFRP-3A	29.4	300	0	750	682	Rec	750	1365	2.00	G	Ct	U	1	1	90	3.900	26100	575	0.0220	0.0260
102	(Long and Marian, 2015)	G2-CFRP-3	29.4	300	0	750	682	Rec	750	1365	2.00	C	Ct	U	1	1	90	3.000	95800	986	0.0103	0.0200
103	(Bousselham and Chaallal., 2013)	ED1-S1-2L	25.0	152	508	406	350	T	304	1050	3.00	C	Ct	U	1	1	90	0.204	231000	3650	0.0158	0.0027
104	(Gonzalez-Libreros et al., 2017)	S2-FRP-F1-UN	23.3	150	0	300	230	Rec	300	750	3.26	C	Ct	U	1	1	90	0.165	390000	3000	0.0077	0.0022
105	(G.M.Chen et al.,2016)	S8U	46.0	200	500	400	320	T	300	960	3.00	C	Dt	U	50	100	90	0.167	226000	4361	0.0193	0.0008
106	(G.M.Chen et al.,2016)	S8UFA1	46.0	200	500	400	320	T	300	960	3.00	C	Dt	U+	50	100	90	0.167	226000	4361	0.0193	0.0008
107	(G.M.Chen et al.,2016)	S8UFA2	46.0	200	500	400	320	T	300	960	3.00	C	Dt	U+	50	100	90	0.167	226000	4361	0.0193	0.0008
108	(G.M.Chen et al.,2016)	S8UEA1	46.0	200	500	400	320	T	300	960	3.00	C	Dt	U+	50	100	90	0.167	226000	4361	0.0193	0.0008
109	(Belarbi et al. 2012)	RC-8-S90-NA	20.7	457	1067	940	830	T	762	2880	3.47	C	Dt	U	254	381	90	0.130	228000	3792	0.0166	0.0004
110	(Belarbi et al. 2012)	RC-8-S90-DMA	23.8	457	1067	940	830	T	762	2880	3.47	C	Dt	U+	254	381	90	0.130	228000	3792	0.0166	0.0004
111	(Belarbi et al. 2012)	RC-12-S90-NA	28.9	457	1067	940	830	T	762	2880	3.47	C	Dt	U	254	381	90	0.130	228000	3792	0.0166	0.0004
112	(Belarbi et al. 2012)	RC-12-S90-DMA	30.5	457	1067	940	830	T	762	2880	3.47	C	Dt	U+	254	381	90	0.130	228000	3792	0.0166	0.0004
113	(Belarbi et al. 2012)	RC-12-S90-SDMA-PC	20.0	457	1067	940	831	T	762	2880	3.47	C	Dt	U+	254	381	90	0.130	228000	3792	0.0166	0.0004

No	References	Specimens ID	Longitudinal Reinforcement				Steel stirrups							Test results				
			Esl (Mpa)	fyl (Mpa)	Asl (mm2)	ρsl	Type	Diameter (mm)	Spacing (mm)	Es (MPa)	fy (MPa)	As (mm2)	ρs	Vu, test	Mode of Failure	Vf, test	Vc+Vs, test	Vf gain %
71	(Grande et al., 2013)	RS3UL3	210000	476	2148.8	0.0226	Deformed	8	300	210000	476	100.53	0.0013	270.0	DB	110	160	68.8
72	(Grande et al., 2013)	RS2UL3	210000	476	2148.8	0.0226	Deformed	8	200	210000	476	100.53	0.0020	280.0	DB	65	215	30.2
73	(Grande et al., 2013)	RS4UL3	210000	476	2148.8	0.0226	Deformed	8	400	210000	476	100.53	0.0010	225.0	DB	100	125	80.0
74	(Grande et al., 2013)	RS4UL4	210000	476	2148.8	0.0226	Deformed	8	400	210000	476	100.53	0.0010	200.0	DB	60	140	42.9
75	(Koutas and Triantafillou, 2013)	U2C	210000	546	1017.9	0.0278	Deformed	8	100	200000	548	100.53	0.0072	103.0	DB	29	74	39.2
76	(Koutas and Triantafillou, 2013)	U2C-AN3Ch+	210000	546	1017.9	0.0278	Deformed	8	100	200000	548	100.53	0.0072	111.0	DB	37	74	50.0
77	(Koutas and Triantafillou, 2013)	U2C-AN3Cin+	210000	546	1017.9	0.0278	Deformed	8	100	200000	548	100.53	0.0072	150.0	DB	76	74	102.7
78	(Koutas and Triantafillou, 2013)	U2C-AN5Cin+	210000	546	1017.9	0.0278	Deformed	8	100	200000	548	100.53	0.0072	158.0	DB	84	74	113.5
79	(Koutas and Triantafillou, 2013)	U2G-AN3Gin+	210000	546	1017.9	0.0278	Deformed	8	100	200000	548	100.53	0.0072	160.0	DB	86	74	116.2
80	(Azate et al 2013)	U90C5	200000	500	1885.0	0.0212	Deformed	8	380	200000	500	100.53	0.0011	206.0	DB	52	154	33.8
81	(Azate et al 2013)	U90C5	200000	500	1885.0	0.0212	Deformed	8	380	200000	500	100.53	0.0011	232.0	DB	78	154	50.6
82	(Azate et al 2013)	U90S5	200000	500	1885.0	0.0212	Deformed	8	380	200000	500	100.53	0.0011	232.0	DB	78	154	50.6
83	(Azate et al 2013)	U90S5	200000	500	1885.0	0.0212	Deformed	8	380	200000	500	100.53	0.0011	230.0	DB	76	154	49.4
84	(Azate et al 2013)	U90C3	200000	500	1885.0	0.0212	Deformed	8	380	200000	500	100.53	0.0011	212.0	DB	58	154	37.7
85	(Azate et al 2013)	U90C3	200000	500	1885.0	0.0212	Deformed	8	380	200000	500	100.53	0.0011	203.0	DB	49	154	31.8
86	(Azate et al 2013)	U90S3	200000	500	1885.0	0.0212	Deformed	8	380	200000	500	100.53	0.0011	202.0	DB	48	154	31.2
87	(Azate et al 2013)	U90S3	200000	500	1885.0	0.0212	Deformed	8	380	200000	500	100.53	0.0011	214.0	DB	60	154	39.0
88	(Azate et al 2013)	U90S3	200000	500	1885.0	0.0212	Deformed	8	380	200000	500	100.53	0.0011	206.0	DB	52	154	33.8
89	(Azate et al 2013)	U45S5	200000	500	1885.0	0.0212	Deformed	8	380	200000	500	100.53	0.0011	214.0	DB	60	154	39.0
90	(Azate et al 2013)	U45S3	200000	500	1885.0	0.0212	Deformed	8	380	200000	500	100.53	0.0011	194.0	DB	40	154	26.0
91	(Azate et al 2013)	U45S3	200000	500	1885.0	0.0212	Deformed	8	380	200000	500	100.53	0.0011	209.0	DB	55	154	35.7
92	(Shamim Sheikh 2014)	S5-US	214000	481	5654.9	0.0259	Deformed	10	500	195000	501	157.08	0.0008	518.0	DB	103	415	24.8
93	(Shamim Sheikh 2014)	S5-UA	214000	481	5654.9	0.0259	Deformed	10	500	195000	501	157.08	0.0008	622.0	DB	207	415	49.9
94	(Shamim Sheikh 2014)	S2-US	214000	481	5654.9	0.0259	Deformed	10	250	195000	501	157.08	0.0016	629.0	DB	78	551	14.2
95	(Shamim Sheikh 2014)	S2-UA	214000	481	5654.9	0.0259	Deformed	10	250	195000	501	157.08	0.0016	688.0	DB	137	551	24.9
96	(Karzad, 2015)	SU-SS-2L-36	200000	600	2323.1	0.0306	Deformed	8	150	200000	490	100.53	0.0029	230.0	DB	55	175	31.4
97	(Karzad, 2015)	SU-SS-2L-36	200000	600	2323.1	0.0306	Deformed	8	150	200000	490	100.53	0.0029	217.0	DB	42	175	24.0
98	(Long and Marian, 2015)	G1-GFRP3	200000	420	2777.2	0.0176	Deformed	8	180	200000	350	100.53	0.0019	459.5	DB	65	394.5	16.5
99	(Long and Marian, 2015)	G2-GFRP-2A	200000	420	2082.9	0.0236	Deformed	8	320	200000	350	100.53	0.0016	305.0	DB	80	225	35.6
100	(Long and Marian, 2015)	G2-CFRP-2	200000	420	2082.9	0.0236	Deformed	8	320	200000	350	100.53	0.0016	345.0	DB	120	225	53.3
101	(Long and Marian, 2015)	G2-GFRP-3A	200000	420	4908.7	0.0240	Deformed	8	320	200000	350	100.53	0.0010	650.0	DB	180	470	38.3
102	(Long and Marian, 2015)	G2-CFRP-3	200000	420	4908.7	0.0240	Deformed	8	320	200000	350	100.53	0.0010	730.0	DB	260	470	55.3
103	(Bousselham and Chaallal., 2013)	ED1-S1-2L	200000	480	1963.5	0.0369	Deformed	8	175	215000	645	100.53	0.0038	267.0	shear	24.4	242.6	10.1
104	(Gonzalez-Libreros et al., 2017)	S2-FRP-F1-UN	200000	545	2123.7	0.0616	Deformed	8	200	200000	535	100.53	0.0034	169.2	DB	39.6	129.6	30.6
105	(G.M.Chen et al.,2016)	S8U	194000	416	2463.0	0.0385	Deformed	8	200	194000	416	100.53	0.0025	300.8	DB	29.871	270.949	11.0
106	(G.M.Chen et al.,2016)	S8UFA1	194000	416	2463.0	0.0385	Deformed	8	200	194000	416	100.53	0.0025	321.0	DB	49.88	271.11	18.4
107	(G.M.Chen et al.,2016)	S8UFA2	194000	416	2463.0	0.0385	Deformed	8	200	194000	416	100.53	0.0025	366.3	DB	95.14	271.11	35.1
108	(G.M.Chen et al.,2016)	S8UEA1	194000	416	2463.0	0.0385	Deformed	8	200	194000	416	100.53	0.0025	361.9	DB	90.75	271.11	33.5
109	(Belarbi et al. 2012)	RC-8-S90-NA	200000	414	12214.5	0.0322	Deformed	10	200	200000	276	157.08	0.0017	838.0	DB	182.4	655.6	27.8
110	(Belarbi et al. 2012)	RC-8-S90-DMA	200000	414	12214.5	0.0322	Deformed	10	200	200000	276	157.08	0.0017	890.0	DB	172.0	718	24.0
111	(Belarbi et al. 2012)	RC-12-S90-NA	200000	414	12214.5	0.0322	Deformed	10	300	200000	276	157.08	0.0011	696.0	DB	176.0	520	33.8
112	(Belarbi et al. 2012)	RC-12-S90-DMA	200000	414	12214.5	0.0322	Deformed	10	300	200000	276	157.08	0.0011	816.0	DB	243.0	573	42.4
113	(Belarbi et al. 2012)	RC-12-S90-SDMA-PC	200000	414	12214.5	0.0322	Deformed	10	300	200000	276	157.08	0.0011	961.0	RT	262.0	699	37.5

No	References	Specimens ID	Concrete strength	Beam dimension and properties								EB-FRP shear strengthening										
			fc (MPa)	bw (mm)	bf(T) (mm)	h (mm)	d (mm)	Cross Section	hfrp (mm)	Shear Span (a)	a/d	Type	Distri-bution	Wrapping Scheme	wf (mm)	Sf (mm)	Inclination β(°)	tf (mm)	Ef (MPa)	ff (MPa)	ε_f	ρf
114	(Sato et al., 1996)	S6	39.7	200	0	300	260	Rec	300	700	2.69	C	Ct	U	1	1	90	0.110	230000	3473	0.0151	0.0011
115	(Taerwe et al., 1997)	BS2	35.1	200	0	450	420	Rec	450	1250	2.98	C	Dt	U	50	400	90	0.110	279520	3494	0.0125	0.0001
116	(Taerwe et al., 1997)	BS5	36.8	200	0	450	420	Rec	450	1250	2.98	C	Dt	U	50	400	90	0.110	279520	3494	0.0125	0.0001
117	(Taerwe et al., 1997)	BS6	35.8	200	0	450	420	Rec	450	1250	2.98	C	Dt	U	50	400	90	0.110	279520	3494	0.0125	0.0001
118	(Matthys, 2000)	BS5	36.0	200	0	450	390	Rec	450	1250	3.21	C	Dt	U	50	400	90	0.110	233000	3500	0.0150	0.0001
119	(Deniaud and Cheng, 2001)	T6S4-C90	44.1	140	400	600	540	T	450	1480	2.74	C	Dt	U	50	100	90	0.110	230000	3400	0.0148	0.0008
120	(Deniaud and Cheng, 2001)	T6S4-G90	44.1	140	400	600	540	T	450	1480	2.74	G	Ct	U	1	1	90	1.800	17700	106	0.0060	0.0257
121	(Park et al., 2001)	5	25.4	100	300	300	230	T	250	810	3.52	C	Ct	U	1	1	90	0.160	240000	3400	0.0142	0.0032
122	(Park et al., 2001)	6	25.4	100	300	300	230	T	250	810	3.52	G	Dt	U	25	75	90	1.200	155000	2400	0.0155	0.0080
123	(Deniaud and Cheng, 2003)	T4S4-G90	30.0	140	400	400	340	T	250	1030	3.03	G	Ct	U	1	1	90	1.800	17700	106	0.0060	0.0257
124	(Deniaud and Cheng, 2003)	T4S2-G90	30.3	140	400	400	340	T	250	1030	3.03	G	Ct	U	1	1	90	1.800	17700	106	0.0060	0.0257
125	(Deniaud and Cheng, 2003)	T4S2-Tri	30.4	140	400	400	340	T	250	1030	3.03	G	Ct	U	1	1	60	2.100	8100	124	0.0153	0.0300
126	(Diagana et al., 2003)	PU1	38.0	130	0	450	425	Rec	450	900	2.12	C	Dt	U	40	200	90	0.430	105000	1400	0.0133	0.0013
127	(Diagana et al., 2003)	PU2	38.0	130	0	450	425	Rec	450	900	2.12	C	Dt	U	40	250	90	0.430	105000	1400	0.0133	0.0011
128	(Diagana et al., 2003)	PU3	38.0	130	0	450	425	Rec	450	900	2.12	C	Dt	U	40	300	45	0.430	105000	1400	0.0133	0.0009
129	(Diagana et al., 2003)	PU4	38.0	130	0	450	425	Rec	450	900	2.12	C	Dt	U	40	350	45	0.430	105000	1400	0.0133	0.0008
130	(Xuesong and Zhongfan, 2004)	SB1-3	32.8	150	0	360	300	Rec	360	864	2.88	C	Ct	U	1	1	90	0.220	235000	4200	0.0179	0.0029
131	(Xuesong and Zhongfan, 2004)	SB1-4	32.8	150	0	360	300	Rec	360	864	2.88	C	Ct	U	1	1	90	0.220	235000	4200	0.0179	0.0029
132	(Xuesong and Zhongfan, 2004)	SB1-5	32.8	150	0	360	300	Rec	360	864	2.88	C	Dt	U	40	120	90	0.220	235000	4200	0.0179	0.0010
133	(Xuesong and Zhongfan, 2004)	SB1-6	32.8	150	0	360	300	Rec	360	864	2.88	C	Dt	U	40	120	90	0.220	235000	4200	0.0179	0.0010
134	(Xuesong and Zhongfan, 2004)	SB1-7	32.8	150	0	360	300	Rec	360	864	2.88	C	Dt	U	40	120	90	0.220	235000	4200	0.0179	0.0010
135	(Xuesong and Zhongfan, 2004)	SB1-8	32.8	150	0	360	300	Rec	360	864	2.88	C	Dt	U	40	120	90	0.220	235000	4200	0.0179	0.0010
136	(Xuesong and Zhongfan, 2004)	SB1-9	32.8	150	0	360	300	Rec	360	864	2.88	C	Dt	U	40	120	90	0.440	235000	4200	0.0179	0.0020
137	(Xuesong and Zhongfan, 2004)	SB1-10	32.8	150	0	360	300	Rec	360	864	2.88	C	Dt	U	40	120	90	0.440	235000	4200	0.0179	0.0020
138	(Xuesong and Zhongfan, 2004)	SB2-2	32.8	150	0	360	300	Rec	360	864	2.88	C	Dt	U	40	120	90	0.220	235000	4200	0.0179	0.0010
139	(Xuesong and Zhongfan, 2004)	SB2-3	32.8	150	0	360	300	Rec	360	864	2.88	C	Dt	U	40	120	90	0.220	235000	4200	0.0179	0.0010
140	(Xuesong and Zhongfan, 2004)	SB3-2	32.8	150	0	360	300	Rec	360	864	2.88	C	Dt	U	40	120	90	0.220	235000	4200	0.0179	0.0010
141	(Xuesong and Zhongfan, 2004)	SB3-3	32.8	150	0	360	300	Rec	360	864	2.88	C	Dt	U	40	120	90	0.220	235000	4200	0.0179	0.0010
142	(Dias and Barros, 2006)	2S_7M(2)	31.5	180	450	400	360	T	300	900	2.50	C	Dt	U	60	114	90	0.350	218400	2862	0.0131	0.0020
143	(Dias and Barros, 2006)	4S_4M(1)	31.5	180	450	400	360	T	300	900	2.50	C	Dt	U	60	180	90	0.180	218400	2862	0.0131	0.0007
144	(Dias and Barros, 2006)	4S_7M(1)	31.5	180	450	400	360	T	300	900	2.50	C	Dt	U	60	114	90	0.180	218400	2862	0.0131	0.0011
145	(De Lorenzis and Rizzo, 2006)	UW90	29.3	200	0	210	173	Rec	200	519	3.00	C	Ct	U	1	1	90	0.170	230000	3430	0.0149	0.0017
146	(Altin et al., 2009)	2	25.2	120	360	360	330	T	285	1650	5.00	C	Dt	U	50	125	90	0.120	231000	4100	0.0177	0.0008
147	(Altin et al., 2009)	3	24.9	120	360	360	330	T	285	1650	5.00	C	Dt	U	50	150	90	0.120	231000	4100	0.0177	0.0007
148	(Altin et al., 2009)	4	24.8	120	360	360	330	T	285	1650	5.00	C	Dt	U	50	200	90	0.120	231000	4100	0.0177	0.0005
149	(Gamino et al. 2010)	VTC1	60.5	120	400	300	265	T	220	700	2.64	C	Dt	U	50	150	90	0.130	230000	2730	0.0119	0.0007
150	(Gamino et al. 2010)	VTC2	60.5	120	400	300	265	T	220	700	2.64	C	Dt	U+	60	150	90	0.110	221000	2730	0.0124	0.0007
151	(Gamino et al. 2010)	VTC3	59.6	120	400	300	265	T	220	700	2.64	C	Dt	U	50	150	90	0.170	218900	2730	0.0125	0.0009
152	(Gamino et al. 2010)	VTC4	60.0	120	400	300	265	T	220	700	2.64	C	Dt	U+	50	175	90	0.110	235000	2915	0.0124	0.0005
153	(El-Ghandour, 2011)	B2S	39.5	120	0	300	250	Rec	260	900	3.60	C	Dt	U	50	187.5	90	0.176	240000	3800	0.0158	0.0008
154	(El-Ghandour, 2011)	B3S	39.5	120	0	300	250	Rec	260	900	3.60	C	Dt	U	50	187.5	90	0.176	240000	3800	0.0158	0.0008
155	(El Maaddawy, 2012)	U-EB1	20.0	120	300	240	200	T	190	600	3.00	C	Dt	U	70	120	90	0.381	230000	3450	0.0150	0.0037

No	References	Specimens ID	Longitudinal Reinforcement				Steel stirrups							Test results				
			Esl (Mpa)	fyl (Mpa)	Asl (mm2)	ρsl	Type	Diameter (mm)	Spacing (mm)	Es (MPa)	fy (MPa)	As (mm2)	ρs	Vu, test	Mode of Failure	Vf, test	Vc+Vs, test	Vf gain %
114	(Sato et al., 1996)	S6	180000	371	1701.0	0.0330	Plain	6	120	183000	355	56.55	0.0024	211.2	DB	119.1	92.1	129.3
115	(Taerwe et al., 1997)	BS2	200000	559	1885.0	0.0220	Plain	6	200	200000	559	56.55	0.0014	247.5	DB	41.2	206.3	20.0
116	(Taerwe et al., 1997)	BS5	200000	559	1885.0	0.0220	Plain	6	400	200000	559	56.55	0.0007	170.0	DB	33.4	136.6	24.5
117	(Taerwe et al., 1997)	BS6	200000	559	1885.0	0.0220	Plain	6	400	200000	559	56.55	0.0007	166.6	DB	30	136.6	22.0
118	(Matthys, 2000)	BS5	200000	530	1885.0	0.0242	Plain	6	400	200000	590	56.55	0.0007	170.0	DB	33.4	136.6	24.5
119	(Deniaud and Cheng, 2001)	T6S4-C90	200000	NA	2124.0	0.0280	Plain	6	400	200000	520	56.55	0.0010	272.8	DB	85.2	187.6	45.4
120	(Deniaud and Cheng, 2001)	T6S4-G90	200000	NA	2124.0	0.0280	Plain	6	400	200000	520	56.55	0.0010	297.5	DB	109.9	187.6	58.6
121	(Park et al., 2001)	5	210000	489	668.0	0.0290	Plain	6	75	210000	325	56.55	0.0075	120.1	DB	38	82.1	46.3
122	(Park et al., 2001)	6	210000	489	668.0	0.0290	Plain	6	75	210000	325	56.55	0.0075	107.2	DB	25.1	82.1	30.6
123	(Deniaud and Cheng, 2003)	T4S4-G90	200001	NA	1062.0	0.0210	Plain	6	400	200000	520	56.55	0.0010	205.6	RT	48.6	157	31.0
124	(Deniaud and Cheng, 2003)	T4S2-G90	200003	NA	1062.0	0.0210	Plain	6	200	200000	520	56.55	0.0020	225.6	RT	24.3	201.3	12.1
125	(Deniaud and Cheng, 2003)	T4S2-Tri	200004	NA	1062.0	0.0210	Plain	6	200	200000	520	56.55	0.0020	242.7	RT	41.4	201.3	20.6
126	(Diagana et al., 2003)	PU1	210000	550	710.0	0.0130	Plain	6	300	210000	240	56.55	0.0014	142.5	DB	32.5	110	29.5
127	(Diagana et al., 2003)	PU2	210000	550	710.0	0.0130	Plain	6	300	210000	240	56.55	0.0014	130.0	DB	20	110	18.2
128	(Diagana et al., 2003)	PU3	210000	550	710.0	0.0130	Plain	6	300	210000	240	56.55	0.0014	154.5	DB	44.5	110	40.5
129	(Diagana et al., 2003)	PU4	210000	550	710.0	0.0130	Plain	6	300	210000	240	56.55	0.0014	150.0	DB	40	110	36.4
130	(Xuesong and Zhongfan, 2004)	SB1-3	205000	395	2011.0	0.0450	Plain	6	135	205000	395	56.55	0.0028	240.0	DB	63.5	176.5	36.0
131	(Xuesong and Zhongfan, 2004)	SB1-4	205000	395	2011.0	0.0450	Plain	6	135	205000	395	56.55	0.0028	253.0	DB	76.5	176.5	43.3
132	(Xuesong and Zhongfan, 2004)	SB1-5	205000	395	2011.0	0.0450	Plain	6	135	205000	395	56.55	0.0028	246.0	DB	69.5	176.5	39.4
133	(Xuesong and Zhongfan, 2004)	SB1-6	205000	395	2011.0	0.0450	Plain	6	135	205000	395	56.55	0.0028	230.0	DB	53.5	176.5	30.3
134	(Xuesong and Zhongfan, 2004)	SB1-7	205000	395	2011.0	0.0450	Plain	6	135	205000	395	56.55	0.0028	240.0	DB	63.5	176.5	36.0
135	(Xuesong and Zhongfan, 2004)	SB1-8	205000	395	2011.0	0.0450	Plain	6	135	205000	395	56.55	0.0028	239.0	DB	62.5	176.5	35.4
136	(Xuesong and Zhongfan, 2004)	SB1-9	205000	395	2011.0	0.0450	Plain	6	135	205000	395	56.55	0.0028	240.0	DB	63.5	176.5	36.0
137	(Xuesong and Zhongfan, 2004)	SB1-10	205000	395	2011.0	0.0450	Plain	6	135	205000	395	56.55	0.0028	243.0	DB	66.5	176.5	37.7
138	(Xuesong and Zhongfan, 2004)	SB2-2	205000	395	2011.0	0.0450	Plain	6	135	205000	395	56.55	0.0028	290.0	DB	72	218	33.0
139	(Xuesong and Zhongfan, 2004)	SB2-3	205000	395	2011.0	0.0450	Plain	6	135	205000	395	56.55	0.0028	270.0	DB	52	218	23.9
140	(Xuesong and Zhongfan, 2004)	SB3-2	205000	395	2011.0	0.0450	Plain	6	135	205000	395	56.55	0.0028	310.0	DB	35	275	12.7
141	(Xuesong and Zhongfan, 2004)	SB3-3	205000	395	2011.0	0.0450	Plain	6	135	205000	395	56.55	0.0028	329.0	DB	54	275	19.6
142	(Dias and Barros, 2006)	2S_7M(2)	200000	447	1810.0	0.0280	Plain	6	300	200000	542	56.55	0.0010	191.3	DB	39.8	151.5	26.3
143	(Dias and Barros, 2006)	4S_4M(1)	200000	447	1810.0	0.0280	Plain	6	180	200000	542	56.55	0.0017	250.4	DB	27.6	222.8	12.4
144	(Dias and Barros, 2006)	4S_7M(1)	200000	447	1810.0	0.0280	Plain	6	180	200000	542	56.55	0.0017	253.8	DB	31	222.8	13.9
145	(De Lorenzis and Rizzo, 2006)	UW90	211300	545	1521.0	0.0440	Plain	6	160	251500	665	56.55	0.0018	141.5	DB	19.3	122.2	15.8
146	(Altin et al., 2009)	2	200000	610	942.5	0.0238	Plain	6	300	200000	450	56.55	0.0016	50.7	DB	19.7	31	63.5
147	(Altin et al., 2009)	3	200000	610	942.5	0.0238	Plain	6	300	200000	450	56.55	0.0016	45.8	DB	14.8	31	47.7
148	(Altin et al., 2009)	4	200000	610	942.5	0.0238	Plain	6	300	200000	450	56.55	0.0016	42.3	DB	11.3	31	36.5
149	(Gamino et al. 2010)	VTC1	198000	555	628.3	0.0198	Plain	5	290	188000	517	39.27	0.0011	220.0	DB	37.5	182.5	20.5
150	(Gamino et al. 2010)	VTC2	198000	555	628.3	0.0198	Plain	5	290	188000	517	39.27	0.0011	305.0	RT	80	225	35.6
151	(Gamino et al. 2010)	VTC3	198000	555	628.3	0.0198	Plain	5	290	188000	517	39.27	0.0011	243.0	DB	49	194	25.3
152	(Gamino et al. 2010)	VTC4	198000	555	628.3	0.0198	Plain	5	290	188000	517	39.27	0.0011	275.0	RT	65	210	31.0
153	(El-Ghandour, 2011)	B2S	200000	400	1526.8	0.0509	Plain	6	200	200000	290	56.55	0.0024	112.5	DB	27.5	85	32.4
154	(El-Ghandour, 2011)	B3S	200000	400	804.2	0.0268	Plain	6	200	200000	290	56.55	0.0024	75.0	DB	12.5	62.5	20.0
155	(El Maaddawy, 2012)	U-EB1	200000	520	1383.9	0.0577	Plain	6	120	200000	344	56.55	0.0039	104.0	DB	15	89	16.9

No	References	Specimens ID	Concrete strength	Beam dimension and properties								EB-FRP shear strengthening										
			fc (MPa)	bw (mm)	bf(T) (mm)	h (mm)	d (mm)	Cross Section	hfrp (mm)	Shear Span (a)	a/d	Type	Distri-bution	Wrapping Scheme	wf (mm)	Sf (mm)	Inclination β(°)	tf (mm)	Ef (MPa)	ff (MPa)	ε_f	ρf
156	(El Maaddawy, 2012)	U-EB2	20.0	120	300	240	200	T	190	600	3.00	C	Dt	U	70	120	90	0.381	230000	3450	0.0150	0.0037
157	(El Maaddawy, 2012)	D-EB1-PAF	20.0	120	300	240	200	T	190	600	3.00	C	Dt	U+	70	120	90	0.381	230000	3450	0.0150	0.0037
158	(El Maaddawy, 2012)	D-EB2-PAF	20.0	120	300	240	200	T	190	600	3.00	C	Dt	U+	70	120	90	0.381	230000	3450	0.0150	0.0037
159	(El Maaddawy, 2012)	D-EB1-TB	20.0	120	300	240	200	T	190	600	3.00	C	Dt	U+	70	120	90	0.381	230000	3450	0.0150	0.0037
160	(El Maaddawy, 2012)	D-EB2-TB	20.0	120	300	240	200	T	190	600	3.00	C	Dt	U+	70	120	90	0.381	230000	3450	0.0150	0.0037
161	(Bagio et al., 2014)	Beam 2	50.1	150	0	350	295	Rec	350	900	3.05	C	Dt	U	200	275	90	0.381	230000	3059	0.0133	0.0037
162	(Bagio et al., 2014)	Beam 3	50.1	150	0	350	295	Rec	300	900	3.05	C	Dt	U+	200	275	90	0.381	230000	3059	0.0133	0.0037
163	(Bagio et al., 2014)	Beam 6	50.1	150	0	350	295	Rec	350	900	3.05	G	Dt	U	100	200	90	0.508	26000	546	0.0210	0.0034
164	(Bagio et al., 2014)	Beam 7	50.1	150	0	350	295	Rec	300	900	3.05	G	Dt	U	100	200	90	0.508	26000	546	0.0210	0.0034
165	(Karzad, 2015)	RB-2L-0.50-S-a	40.0	230	0	390	330	Rec	390	1150	3.48	C	Dt	U	100	150	90	0.332	230000	4900	0.0213	0.0019
166	(Karzad, 2015)	RB-2L-0.50-S-b	40.0	230	0	390	330	Rec	390	1150	3.48	C	Dt	U	100	150	90	0.332	230000	4900	0.0213	0.0019
167	(Karzad, 2015)	SB-2L-0.50-S	33.0	230	0	390	330	Rec	390	1150	3.48	C	Dt	U	100	150	90	0.332	230000	4900	0.0213	0.0019
168	(Karzad, 2015)	RS-S-1L-30	30.0	230	0	390	330	Rec	390	1150	3.48	C	Dt	U	100	150	90	0.165	230000	4900	0.0213	0.0010
169	(Karzad, 2015)	RS-S-2L-38	38.0	230	0	390	330	Rec	390	1150	3.48	C	Dt	U	100	150	90	0.332	230000	4900	0.0213	0.0019
170	(Karzad, 2015)	RS-S-2L-38	38.0	230	0	390	330	Rec	390	1150	3.48	C	Dt	U	100	150	90	0.332	230000	4900	0.0213	0.0019
171	(Karzad, 2015)	SU-S-2L-30	30.0	230	0	390	330	Rec	390	1150	3.48	C	Dt	U	100	150	90	0.332	230000	4900	0.0213	0.0019
172	(Karzad, 2015)	SU-S-2L-34	34.0	230	0	390	330	Rec	390	1150	3.48	C	Dt	U	100	150	90	0.332	230000	4900	0.0213	0.0019
173	(Long and Marian, 2015)	G1-GFRP1	31.2	100	0	200	175	Rec	200	300	1.71	G	Ct	U	1	1	90	1.300	26100	575	0.0220	0.0260
174	(Long and Marian, 2015)	G1-GFRP2	31.2	200	0	400	350	Rec	400	595	1.70	G	Ct	U	1	1	90	2.600	26100	575	0.0220	0.0260
175	(Long and Marian, 2015)	G2-GFRP-1A	29.4	100	0	250	196	Rec	250	400	2.04	G	Ct	U	1	1	90	1.300	26100	575	0.0220	0.0260
176	(Long and Marian, 2015)	G2-CFRP-1	29.4	100	0	250	196	Rec	250	400	2.04	C	Ct	U	1	1	90	1.000	95800	986	0.0103	0.0200
177	(Bousselham and Chaallal., 2013)	ED2-S1-2L	25.0	95	270	220	175	T	165	525	3.00	C	Ct	U	1	1	90	0.132	231000	3650	0.0158	0.0028
178	(Oller et al., 2019)	M1B	33.0	200	600	550	493	T	400	1480	3.00	C	Dt	U+	50	240	90	0.170	230000	3400	0.0148	0.0004
179	(Oller et al., 2019)	M2B	33.0	200	600	550	493	T	400	1480	3.00	C	Dt	U+	100	240	90	0.170	230000	3400	0.0148	0.0007
180	(Oller et al., 2019)	H2A	38.0	200	600	550	493	T	400	1480	3.00	C	Dt	U+	100	240	90	0.170	230000	3400	0.0148	0.0007
181	(Oller et al., 2019)	H2B	38.0	200	600	550	493	T	400	1480	3.00	C	Dt	U+	100	240	90	0.170	230000	3400	0.0148	0.0007
182	(Oller et al., 2019)	H3A	38.0	200	600	550	493	T	400	1480	3.00	C	Ct	U+	1	1	90	0.170	230000	3400	0.0148	0.0017
183	(Oller et al., 2019)	H3B	38.0	200	600	550	493	T	400	1480	3.00	C	Ct	U+	1	1	90	0.170	230000	3400	0.0148	0.0017
184	(Said Allam 2003)	US-1	32.0	120	0	200	175	Rec	200	450	2.57	C	Dt	U	50	100	90	0.260	230000	3500	0.0152	0.0022
185	(Said Allam 2003)	US-2	32.0	120	0	200	175	Rec	200	450	2.57	C	Dt	U	50	100	90	0.260	230000	3500	0.0152	0.0022
186	(Said Allam 2003)	US-3	32.0	120	0	200	175	Rec	200	450	2.57	C	Dt	U	50	100	90	0.260	230000	3500	0.0152	0.0022
187	(Said Allam 2003)	US-4	32.0	120	0	200	175	Rec	200	450	2.57	C	Dt	U	50	100	90	0.260	230000	3500	0.0152	0.0022
188	(Zhou et al., 2019)	EB-1-0	22.0	200	0	370	297	Rec	370	600	2.02	C	Dt	U	36	120	90	0.167	270000	4104	0.0152	0.0005
189	(Zhou et al., 2019)	HB-1-3	22.0	200	0	370	297	Rec	370	600	2.02	C	Dt	U+	36	120	90	0.167	270500	4104	0.0152	0.0005
190	(Zhou et al., 2019)	HB-1-6	22.0	200	0	370	297	Rec	370	600	2.02	C	Dt	U+	36	120	90	0.167	270500	4104	0.0152	0.0005
191	(Zhou et al., 2019)	HB-1-12	22.0	200	0	370	297	Rec	370	600	2.02	C	Dt	U+	36	120	90	0.167	270500	4104	0.0152	0.0005

No	References	Specimens ID	Longitudinal Reinforcement				Steel stirrups							Test results				
			Esl (Mpa)	fyl (Mpa)	Asl (mm2)	ρsl	Type	Diameter (mm)	Spacing (mm)	Es (MPa)	fy (MPa)	As (mm2)	ρs	Vu, test	Mode of Failure	Vf, test	Vc+Vs, test	Vf gain %
156	(El Maaddawy, 2012)	U-EB2	200000	520	1383.9	0.0577	Plain	6	120	200000	344	56.55	0.0039	102.0	DB	13	89	14.6
157	(El Maaddawy, 2012)	D-EB1-PAF	200000	520	1383.9	0.0577	Plain	6	120	200000	344	56.55	0.0039	104.0	DB	23	81	28.4
158	(El Maaddawy, 2012)	D-EB2-PAF	200000	520	1383.9	0.0577	Plain	6	120	200000	344	56.55	0.0039	104.0	DB	22	82	26.8
159	(El Maaddawy, 2012)	D-EB1-TB	200000	520	1383.9	0.0577	Plain	6	120	200000	344	56.55	0.0039	122.0	RT	46	76	60.5
160	(El Maaddawy, 2012)	D-EB2-TB	200000	520	1383.9	0.0577	Plain	6	120	200000	344	56.55	0.0039	120.0	RT	36	84	42.9
161	(Bagio et al., 2014)	Beam 2	200000	475	1413.7	0.0319	Plain	6	180	200000	384	56.55	0.0021	186.0	Flexural	25	161	15.5
162	(Bagio et al., 2014)	Beam 3	200000	475	1413.7	0.0319	Plain	6	180	200000	384	56.55	0.0021	195.0	Flexural	34	161	21.1
163	(Bagio et al., 2014)	Beam 6	200000	475	1413.7	0.0319	Plain	6	180	200000	384	56.55	0.0021	167.0	DB	55.5	111.5	49.8
164	(Bagio et al., 2014)	Beam 7	200000	475	1413.7	0.0319	Plain	6	180	200000	384	56.55	0.0021	152.5	DB	41	111.5	36.8
165	(Karzad, 2015)	RB-2L-0.50-S-a	200000	600	2323.1	0.0306	Plain	6	200	200000	290	56.55	0.0012	292.0	DB	95	197	48.2
166	(Karzad, 2015)	RB-2L-0.50-S-b	200000	600	2323.1	0.0306	Plain	6	200	200000	290	56.55	0.0012	295.0	DB	99	196	50.5
167	(Karzad, 2015)	SB-2L-0.50-S	200000	600	2323.1	0.0306	Plain	6	200	200000	290	56.55	0.0012	213.0	DB	87	126	69.0
168	(Karzad, 2015)	RS-S-1L-30	200000	600	2323.1	0.0306	Plain	6	200	200000	290	56.55	0.0012	175.0	DB	74	101	73.3
169	(Karzad, 2015)	RS-S-2L-38	200000	600	2323.1	0.0306	Plain	6	200	200000	290	56.55	0.0012	252.0	DB	113	139	81.3
170	(Karzad, 2015)	RS-S-2L-38	200000	600	2323.1	0.0306	Plain	6	200	200000	290	56.55	0.0012	284.0	DB	145	139	104.3
171	(Karzad, 2015)	SU-S-2L-30	200000	600	2323.1	0.0306	Plain	6	200	200000	290	56.55	0.0012	187.0	DB	86	101	85.1
172	(Karzad, 2015)	SU-S-2L-34	200000	600	2323.1	0.0306	Plain	6	200	200000	290	56.55	0.0012	210.0	DB	98	112	87.5
173	(Long and Marian, 2015)	G1-GFRP1	200000	420	307.9	0.0176	Plain	6	300	200000	350	56.55	0.0019	57.0	DB	18.5	38.5	48.1
174	(Long and Marian, 2015)	G1-GFRP2	200000	420	1256.6	0.0180	Plain	6	150	200000	350	56.55	0.0019	226.5	DB	56.5	170	33.2
175	(Long and Marian, 2015)	G2-GFRP-1A	200000	420	465.0	0.0237	Plain	6	350	200000	350	56.55	0.0016	62.5	DB	17.5	45	38.9
176	(Long and Marian, 2015)	G2-CFRP-1	200000	420	465.0	0.0237	Plain	6	350	200000	350	56.55	0.0016	70.0	DB	25	45	55.6
177	(Bousselham and Chaallal., 2013)	ED2-S1-2L	200000	438	559.2	0.0360	Plain	4.8	100	165000	545	36.19	0.0038	105.1	shear	12.2	92.9	13.1
178	(Oller et al., 2019)	M1B	196121	572	1608.5	0.0163	Plain	6	240	189956	645.73	56.55	0.0012	335.8	DB	65	270.8	24.0
179	(Oller et al., 2019)	M2B	196121	572	1608.5	0.0163	Plain	6	240	189956	645.73	56.55	0.0012	348.0	DB	76	272	27.9
180	(Oller et al., 2019)	H2A	175084	603	2060.9	0.0209	Plain	6	240	189956	645.73	56.55	0.0012	402.9	DB	77.5	325.4	23.8
181	(Oller et al., 2019)	H2B	175084	603	2060.9	0.0209	Plain	6	240	189956	645.73	56.55	0.0012	402.9	DB	56.7	346.2	16.4
182	(Oller et al., 2019)	H3A	175084	603	2060.9	0.0209	Plain	6	240	189956	645.73	56.55	0.0012	382.2	DB	161.1	221.1	72.9
183	(Oller et al., 2019)	H3B	175084	603	2060.9	0.0209	Plain	6	240	189956	645.73	56.55	0.0012	382.2	DB	123.4	258.8	47.7
184	(Said Allam 2003)	US-1	200000	400	603.2	0.0287	Plain	6	120	200000	280	56.55	0.0039	115.0	DB	35.0	80	43.8
185	(Said Allam 2003)	US-2	200000	400	603.2	0.0287	Plain	6	120	200000	280	56.55	0.0039	87.5	DB	25.0	62.5	40.0
186	(Said Allam 2003)	US-3	200000	400	603.2	0.0287	Plain	6	120	200000	280	56.55	0.0039	86.2	DB	23.7	62.5	37.9
187	(Said Allam 2003)	US-4	200000	400	603.2	0.0287	Plain	6	120	200000	280	56.55	0.0039	85.0	DB	22.5	62.5	36.0
188	(Zhou et al., 2019)	EB-1-0	208000	491	2463.0	0.0415	Plain	6.5	120	201000	398	66.37	0.0028	261.0	DB	38.5	222.5	17.3
189	(Zhou et al., 2019)	HB-1-3	208000	491	2463.0	0.0415	Plain	6.5	120	201000	397.8	66.37	0.0028	292.2	DB	30.2	262	11.5
190	(Zhou et al., 2019)	HB-1-6	208000	491	2463.0	0.0415	Plain	6.5	120	201000	397.8	66.37	0.0028	302.1	DB	33.4	268.7	12.4
191	(Zhou et al., 2019)	HB-1-12	208000	491	2463.0	0.0415	Plain	6.5	120	201000	397.8	66.37	0.0028	325.1	RT	45.7	279.4	16.4